Research Article

Benzophenone based photostable fluorescent monoazo disperse dyes: Synthesis, AIE, viscosity, UPF and TD-DFT study

Suvidha S. Shinde[1] · **Amol G. Jadhav**[1] · **Nagaiyan Sekar**[1] (iD)

Abstract

Synthesis of a parallel series of hydrophobic azo dyes (4-hydroxy benzophenone and corresponding 4-methoxy benzophenone series) and a comprehensive systematic spectroscopic study in solvents of varying polarity and viscosity is presented. This includes glycerol-dimethylsulfoxide, toluene–polyethylene glycol 400 and toluene–paraffin oil viscous mixtures. Emission intensities of dyes (hydrazone forms) were enhanced by 47–96 folds in viscous solvent media compared to the non-viscous media. So, role of hydrogen bonding in the emission enhancement were verified for 4-hydroxy benzophenone series with 4-methoxy benzophenone series. Polarity alteration effect on spectroscopic properties of dyes in various viscous combinations has been correlated by solvent polarity graphs. Density Functional Theory (DFT), Time Dependent Density Functional Theory (TD-DFT), HOMO–LUMO energy gap and Electrophilicity-index estimations are in good contract with the experimental interpretations. Dyes on PET fibers showed excellent light fastness. Moreover, all the dyes on dyed fabrics exhibited good sublimation fastness and color values. Ultraviolet A/Ultraviolet B blocking and Ultraviolet Protection Factor (UPF) of all the dyes range 15–50 and are in good agreement with light fastness.

1 Introduction

Azo dyes established as one of the leading dyestuff of industrial colorants [1]. Benzophenone is a well-known aromatic ketone obtained by organic synthesis or from natural products [2]. Benzophenone based compounds have wide applications as excellent UV absorbers [3] and thermal stabilizers [4]. Benzophenone based textile dyes are also well reported [5–7]. To attain the excellent photostability and hence light fastness property different approaches have been made [7–9]. In some cases, fabric dyed with commercially available disperse dyes disperse yellow 86 [10], Disperse Yellow GLFS [11], CI Disperse Yellow 42 [12], 2,4-dihydroxy benzophenone and 4-hydroxy benzophenone were directly applied as UV absorber in the dyeing liquid or by conducting treatment to the dyed fabrics after dyeing [13]. Freeman et al. was the first to investigate the consequence of incorporation of photo-stabilizer moiety into Disperse Yellow 42 in 1992 [14]. Further lot of efforts have been focussed to increase light fastness of dyes by incorporating photo stabilising unit [7, 15, 16]. Also enhancement of the light fastness value is considered to be an important criteria in the textile industry, since Polyethylene Terephthalate (PET) fabrics are extensively used in coloured automobile stuffing, which can be visible to direct sunlight above 50 °C

✉ Nagaiyan Sekar, nethi.sekar@gmail.com; n.sekar@ictmumbai.edu.in | [1]Department of Dyestuff Technology, Institute of Chemical Technology, Nathalal Parekh Marg, Matunga, Mumbai 400 019, India.

[17]. In order to minimize the above said problems, textiles can be served to create sunblind sun umbrella and other shielding clothing. Compared to cosmetics, clothing can be considered as relatively appropriate barrier against UV radiations [18]. So, there is a need to design light fast fluorescent disperse dyes for light energy dissipations [19, 20].

Fluorescent dyes are having great significance in the colouring of synthetic fabrics (e.g. polyacrylonitrile, polyester and polyamides) [19]. Some of the important fluorescent textile dyes (usually disperse dyes) were applied on PET and thus can be considered as important disperse class of dyes [20]. Most of the commercial dyes are yellow, providing the very similar greenish-yellow fluorescent colour which allowed the dyed materials to be more bright, visible and simply noticeable and thus, very commonly encountered on garments worn for safety purposes [21]. The most important fluorescent disperse dyes are C.I. Disperse Yellows 82,184,186 and 232 and C.I. Disperse reds 277, 374. The commercially available fluorescent dyes for textile application are frequently objected for light fastness stability and most of them are incompatible with standards essential for the additional demanding applications [22].

It is reported in the literature that benzophenone and some of it's derivatives are emissive in nature [23–26]. Recently, Barsotti et al. have done wide-ranging work on 4-hydroxy benzophenone for it's fluorescence properties [23, 27]. In general emission properties of azobenzene dyes were induced or altered by various ways which include restricted isomerisation and rotations across –N=N– group by N-B bond formation [28], by incorporation of benzothiazole fluorescent moiety to the azo dyes [29, 30], by cooling of dye sample to very low temperature or by embedding dyes in rigid solvents [31]. However, there are very few fluorescent azobenzenes reported so far [28, 32–37]. Considering decent π-conjugation [38] and restricted rotations across –N=N– group [28], these benzophenone dyes can perform as good applicants for preparation of attractive photo stable fluorescent compounds.

Recently, effect of viscosity on fluctuating emission properties of some of the organic dyes were provided and studied in the literature [39, 40], however, only few reports were based on viscosity effects on the properties of azo dyes [20, 41, 42]. Intramolecular rotation in azo dyes are restricted due to either chemical interaction or adhesion of dyes on fabrics during dyeing [43, 44]. So, it is important to consider intramolecular rotation contributed to the reduction mechanism for the dye in the solution [43]. Although azo-dyes are considered to be non-fluorescent specifically in solutions, but few of them became fluorescent when bound to the substrate [31]. Some of the mono-azo dyes can act as molecular rotors, where fluorescence emission property is sensitive to solution [45]. Some of the

azo dyes were reported with respect to emission intensity enhancement as viscosity of the solution increases [45]. This varying emission characteristics of azo dyes might be described on the basis of constrained rotational motion across the bonds by viscosity in the micro-environment around the molecule [45]. Briefly, it can be suggested that the either viscous micro-environment or the substrate (e.g. fibers) might be responsible for the generation of necessary restriction in azo dyes rotational motions which further contribute to overall emission of these dyes. So, it is of interest to study systematically viscous micro-environmental effects on emission properties of the benzophenone based mono azo disperse dyes.

To meet the requirements of fluorescent disperse dyes with excellent fastness properties, we used the key ingredient benzophenone which acts as a UV stabilizer and it has its own emission, which facilitate to prepare photostable fluorescent dyes. As azo (–N=N–) moiety in azo dyes reduce the fluorescent properties because of photoisomerisation [46, 47] and other dynamics such as excimer or exciplex formation may be contribute to reduce fluorescence [39, 48]. So, to avoid these process and increase fluorescence one can use micro-viscosity as a strategy to make molecule more rigid and restrict its rotations.

Here, we has synthesized a series of benzophenone inbuilt mono azo disperse dyes. Moreover, parallel series of methylated analogues enabled to restricted azohydrazone tautomerization to ensure study of exclusive azo form systematically. Detailed photophysical characterizations were performed to study effect of viscosity, polarity and role of hydrogen bonding in the emission enhancement in these dyes. The dyes are fully characterized in terms of their dyeing properties including the color assessment, sublimation fastness, and light fastness was carried out. Theoretical calculation by DFT supports our experimental outcomes.

2 Experimental section

2.1 Materials and methods

Sodium nitrite, sodium carbonate, sodium hydroxide, aniline, *p*-chloro aniline, *p*-nitro aniline, conc. H_2SO_4, conc. HCl, urea, 4-hydroxy benzophenone, anhydrous methanol, acetone, dimethyl sulphate (DMS), N,N-dimethyl formamide (DMF), Saragen 50 (dispersing agent), sulphamic acid, sodium acetate, sodium chloride and acetic acid procured from Sigma Aldrich India. All A.R. mark organic solvents were procured from SD Fine Chemicals, Mumbai. All organic solvents after distillation as per the standard procedures were utilized further. Melting and boiling points of all the chemicals confirmed and used without any

purifications. Ready for dyeing polyester (PET) (100%) fabric (weight 70 g/m², Ends/105 in. and picks/94 in.), nylon (NYL) (70 d/25 f, plain weaved, 219×191/5 cm), acrylic (ACR) was purchased from Piyush Syndicate, Mumbai. For dyeing application Flexi dyer machine procured from Rossari Labtech Mumbai, India has been used.

Thin layer chromatography on 0.25 mm (silica gel 60F-254 pre-coated aluminum plate) used to check completion of the reactions. Purification of all synthesized compounds accomplished using re-crystallizations technique. Melting point instrument procured from Veego Instruments, Mumbai, India. ¹H-NMR and ¹³C-NMR spectra were documented on Agilent NMR 500 MHz and 125 MHz respectively. Chemical shifts stated in δ-ppm and used CDCl₃ as a solvent and TrimethylSilane (TMS) used as an internal standard. FT-IR spectra noted on JASCO-4100 FT-IR instrument with ATR accessories.

2.2 Photophysical study

Absorption Study of all synthesized dyes documented using Perkin Elmer UV–Vis spectrometer Lambda-25 instrument. Eight unlike polarity solvents used to make 1–5 µM concentration solutions of all dyes (e.g. toluene, 1,4 dioxane, chloroform (CHCl₃), ethyl acetate(EtOAc), methanol (MeOH), tetrahydrofuran (THF), dimethylformamide (DMF) and dimethylsulphoxide (DMSO).

2.3 Viscosity study and calculations

Viscosity sensitivity study was carried out in various polarity viscous mixture such as DMSO—Glycerol, toluene—polyethyleneglycol400 (PEG-400) and toluene-paraffin oil mixture. Varian-Cary Eclipse fluorescence-spectrometer were used to document fluorescence emission spectra of all dyes for this constant concentration 1–5 µM solutions of dyes used. Viscosity (η) of three viscous mixtures at different percentage ratio were mathematically estimated by equation [49] (Table S1).

$$\ln\eta = X1\ \ln\eta1 + X2\ \ln\eta2 \qquad (1)$$

Where,

η = viscosity

X1, X2 = mole fractions of binary mixture (for each constituent separately)

η1, η2 = viscosities of the binary mixture (for each constituent separately)

Varying dynamic viscosity in mPas* against varying solvent ratios in volume % was plotted for three different binary mixtures (i.e. DMSO-Glycerol, toluene-PEG400 and toluene-paraffin oil) (Fig. S1).

2.4 Computational study

DFT computational experiments executed on a HP-workstation XW-8600 with4GB RAM, Xeon processor and Windows Vista as the operating systems. Gaussian 09 W used as the software package [50]. Geometry of ground state optimized by using B3LYP as a functional and 6-311G (d) as a basis set for all the molecules [51, 52]. Oscillator strengths, Vertical excitation energies and orbital contributions (lowest 10 singlet transitions) to the optimized geometry of the ground states of molecules were attained by TD-DFT computations. Polarizable Continuum Model (PCM) implemented for optimizations in various solvent phases in Gaussian 09 [53]. The solvents used in DFT study were toluene, 1,4-dioxane, CHCl₃, EtOAc, MeOH, THF, DMF and DMSO.

2.5 Dyeing study

2.5.1 Color assessment

Color assessment the dyed substrate done on Spectra Scan-5100+ with 10° standard observer under D65illuminant.K/S value of dyed substrate determined by Kubelka-Munk equation.

2.5.2 Fastness property

Dyed samples were tested for light fastness by Q-Sun Xenon Test Chamber (Q-Lab Corporation, Ohio, USA)by AATCC 16/2004 method.

Sublimation fastness tester, RBE Electronics Engineering Private Limited Mumbai, India has been used to evaluate sublimation property of dyed sample by ISO 105-PO1 1993standard method [54].

The change in the shade along with stainings of the in-line fabrics, were evaluated according SDC (Society of Dyers & Colorists) grey scale.

2.5.3 Percentage exhaustion determination

Exhaustion (%) of the of the dye bath were estimated by method [55].

2.5.4 UPF Factor determination

UPF and UVA and UVB percentage transmission estimated by AATCC Test Method-183.Blocking or Transmittance of Erythemally Weighted UV (Ultra-violet)radiations through fabric by AATCC, 2002 (AATCC - Technical Manual, 2015). UV transmittance analyzer was used for the measurements for UPF testing. Measurements were performed using a

UV transmittance UPF Tester V-2000F Fabric Analyzer, Labsphere, US.

2.6 Syntheses and characterization

The synthetic skeleton of synthesized azo dyes **(4a–4c)** **and (5a–5c)** is shown in Scheme 1. Dye **4c** is reported in the literature [56].

2.6.1 Synthesis of azo dyes (4a–4c)

The mixture having aromatic amines (0.003 mol), conc. Hydrochloric acid (HCl) 3 ml (0.035 mol), and 15 ml (1.38 mol) water heated till solution become cleared and this mixture cooled down to 0 °C. The acidity range of the solution determined by using litmus paper. Sodium nitrite 0.25 g (0.003 mol) solution was little by little added in step wise manner with constant stirring at below 5 °C temperature. Further solution permitted to stir for 40 min at 5 °C, after complete addition. Excess nitrous acid quenched by Urea. Meanwhile, sodium hydroxide (0.025 N, 0.003 mol) was dissolved the solution containing 4-hydroxy benzophenone(0.5 g, 0.003 mol)as coupler resulting into clear solution (pH = 11–12). The above diazonium mixture slowly added to the coupler solution with continuous stirring at temperature 0–5 °C. While addition of diazonium salt to the coupler solution pH decreases, so Na_2CO_3 (10% w/v) solution was slowly added to the reaction medium to avoid further decrease in pH and was maintain in between 7.5–8.0 [6]. The further mixture was stirred for 3 h (Scheme 1). The precipitated resultant azo dye filtered and thoroughly washed with water. Recrystallization in ethanol gave desired azo compound. Yield of **4a–4c** after recrystallization was then reported.

2.6.2 Characterizations

4a: Pale yellow powder, Yield–75%, melting point: 130–132 °C.

^{1}H-NMR δ_H (500 MHz,CDCl$_3$): 13.48 (1H, s, −OH), 8.50–8.45 (1H, m, Ar-H), 7.98–7.94 (1H, m, Ar-H), 7.92–7.88 (2H, m, Ar-H), 7.84 (2H, d, J = 8 Hz, Ar-H), 7.66–7.60 (1H, m, Ar-H), 7.55 (2H, d, J = 1 Hz, Ar-H), 7.53 (2H, s, Ar-H), 7.53–7.51 (1H, m, Ar-H), 7.15 (1H, dd, J = 8 Hz and 1 Hz, Ar-H) ppm.

^{13}C-NMR δ_C (125 MHz, CDCl$_3$): 194.7, 156.7, 150.0, 137.8, 136.4, 136.0, 134.9, 132.2, 131.8, 129.7, 129.6, 129.4, 128.4, 122.4, 118.6 ppm.

**FT-IR:** 3057 (phenolic OH), 1680 (C=O), 1644 (C=C), 1275 (C–N) cm^{-1}.

HRMS: 303.1189 (M+H$^+$) (Calculated for $C_{19}H_{15}N_2O_2$: 303.1165).

4b: Pale yellow powder, Yield– 85%, melting point: 204–206 °C.

^{1}H-NMR δ_H (500 MHz,CDCl$_3$): 13.23 (1H, s, −OH), 8.45 (1H, d, J = 2 Hz, Ar-H), 7.96 (1H, dd, J = 8.5 Hz and 2.0 Hz, Ar-H), 7.86 (1H, s, Ar-H), 7.84 (1H, s, Ar-H), 7.83 (1H, s, Ar-H), 7.65–7.60 (2H, m, Ar-H), 7.53 (1H, s, Ar-H), 7.53 (2H, d, J = 2 Hz, Ar-H), 7.51 (1H, s, Ar-H), 7.15 (1H, d, J = 8.5 Hz, Ar-H) ppm.

^{13}C-NMR δ_C (125 MHz, CDCl$_3$): 194.6, 156.6, 148.5, 137.8, 137.7, 136.4, 136.0, 135.1, 132.2, 129.8, 129.8, 129.7, 128.4, 123.6, 118.6 ppm.

Scheme 1 Synthetic scheme of mono azo disperse dyes (**4a–4c** and **5a–5c**)
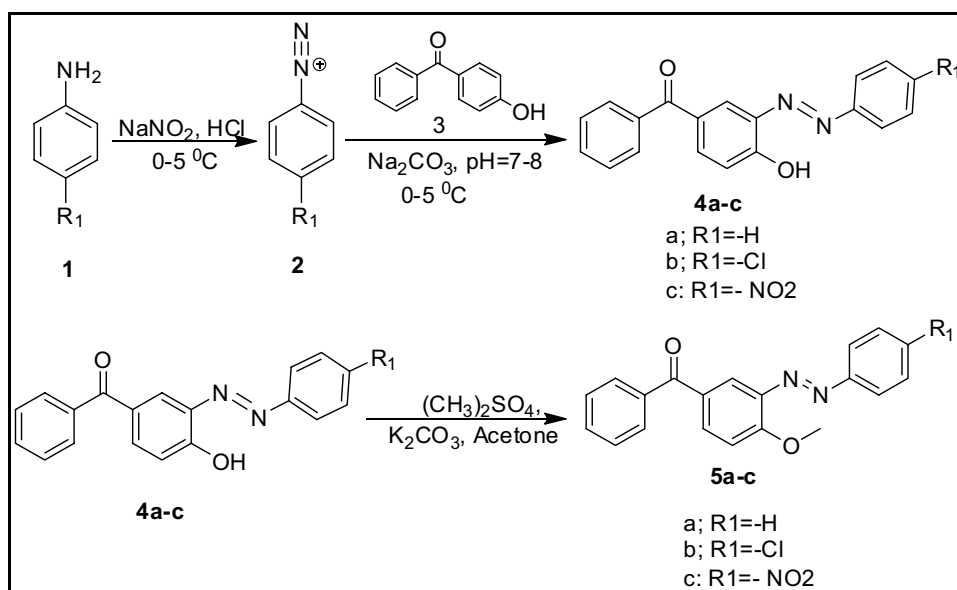
FT-IR: 3063 (phenolic OH), 1691 (C=O), 1652 (C=C), 1284 (C–N), 620 (C–Cl) cm^{-1}.

HRMS: 335.0622 (M–H$^+$) (Calculated for $C_{19}H_{12}ClN_2O_2$: 335.0619).

4c: Pale yellow powder, Yield- 85%, melting point: 194–195 °C.

^{1}H-NMR δ$_H$ (500 MHz, CDCl$_3$): 13.04 (1H, s, –OH), 8.51 (1H, s, Ar-H), 8.41 (2H, d, $J=8.5$ Hz, Ar-H), 8.05 (1H, s, Ar-H), 8.02 (2H, d, $J=9$ Hz, Ar-H), 7.84 (2H, d, $J=7.5$ Hz, Ar-H), 7.64 (1H, t, $J=7.5$ Hz, Ar-H), 7.54 (2H, t, $J=7.5$ Hz, Ar-H), 7.18 (1H, d, $J=8.5$ Hz, Ar-H) ppm.

^{13}C-NMR δ$_C$ (125 MHz, CDCl$_3$): 194.3, 156.5, 153.5, 149.0, 137.5, 137.1, 136.4, 132.8, 132.4, 130.2, 129.7, 128.4, 125.0, 123.0, 118.9 ppm.

FT-IR: 3049 (phenolic OH), 1673 (C=O), 1638 (C=C), 1272 (C–N) cm^{-1}.

HRMS: 346.0848 (M–H$^+$) (Calculated for $C_{19}H_{12}N_3O_2$: 346.0868).

2.6.3 Preparation of methylated forms of azo dyes (5a, 5b, 5c)

General procedure for preparation of azo dyes (5a–5c) Dye **4a**, **4b**, or **4c** was dissolved in acetone along with potassium carbonate (3 eq.) and DMS (0.5 eq.) in 250 ml round bottom flask. The reaction mass was allowed to stirred at 25 °C for 30 min. Reaction was monitored by silica gel TLC. After the starting was consumed, acetone was concentrated under reduce pressure on rota evaporator and solid form thoroughly washed with water and dried. The obtained dyes was pure and single spotted on TLC further no purification is carried out. Therefore, reported yield of **5a**–**c** is in its pure form with very good yields.

2.6.4 Characterizations

5a: Yellow powder, Yield- 96%, melting point: 204 °C.

^{1}H-NMR δ$_H$ (500 MHz, CDCl$_3$): 8.12 (1H, d, $J=2$ Hz, Ar-H), 7.99 (1H, dd, $J=8.5$, 2 Hz, Ar-H), 7.92 (1H, s, Ar-H), 7.91 (1H, s, Ar-H), 7.82 (1H, s, Ar-H), 7.80 (1H, s, Ar-H), 7.60 (1H, t, $J=7.5$ Hz, Ar-H), 7.54–7.48 (5H, m, Ar-H), 7.19 (1H, d, $J=8.5$ Hz, Ar-H), 4.12 (3H, s, –OCH$_3$) ppm.

^{13}C-NMR δ$_C$ (125 MHz, CDCl$_3$): 195.2, 159.9, 152.9, 141.6, 137.8, 134.2, 132.2, 131.2, 130.1, 129.8, 129.1, 128.3, 123.1, 119.4, 112.1, 56.5 ppm.

FT-IR: 1688 (C=O), 1651 (C=C), 1274 (C–N), 1013 (O–CH$_3$) cm^{-1}.

HRMS: 317.1353 (M+H$^+$) (Calculated for $C_{20}H_{17}N_2O_2$: 317.1374).

5b: Yellow powder, Yield –92%, melting point: 163–165 °C.

^{1}H-NMR δ$_H$ (500 MHz, CDCl$_3$): 8.12 (1H, s, Ar-H), 8.00 (1H, d, $J=9$ Hz, Ar-H), 7.87 (2H, d, $J=8.5$ Hz, Ar-H), 7.80 (2H, d, $J=8$ Hz, Ar-H), 7.61 (1H, t, $J=8$ Hz, Ar-H), 7.51 (2H, d, $J=8$ Hz, Ar-H), 7.48 (2H, d, $J=8.5$ Hz, Ar-H), 7.19 (1H, d, $J=8.5$ Hz, Ar-H), 4.12 (3H, s, –OCH$_3$) ppm.

^{13}C-NMR δ$_C$ (125 MHz, CDCl3): 195.2, 16.1, 151.2, 141.4, 137.7, 137.1, 134.5, 132.2, 130.1, 129.8, 129.3, 128.3, 124.3, 119.3, 112.2, 56.6 ppm.

FT-IR: 1694 (C=O), 1661 (C=C), 1283 (C–N), 1008 (O-CH$_3$) cm^{-1}.

HRMS: 351.0955 (M+H$^+$) (Calculated for $C_{20}H_{16}ClN_2O_2$: 351.0965).

5c: Yellow powder, Yield –88%, melting point: 225 °C.

^{1}H-NMR δ$_H$ (500 MHz, CDCl$_3$): 8.39 (1H, s, Ar-H), 8.37 (1H, s, Ar-H), 8.18 (1H, d, $J=2$ Hz, Ar-H), 8.06 (1H, dd, $J=8.5$ Hz and 2 Hz, Ar-H), 8.04 (1H, s, Ar-H), 8.02 (1H, s, Ar-H), 7.81 (2H, d, $J=8.5$ Hz, Ar-H), 7.62 (1H, t, $J=7.5$ Hz, Ar-H), 7.52 (2H, t, $J=7.5$ Hz, Ar-H), 7.23 (1H, d, $J=8.5$ Hz, Ar-H), 4.15 (3H, s, –OCH$_3$) ppm.

^{13}C-NMR δ$_C$ (125 MHz, CDCl3): 195.0, 160.6, 155.9, 148.8, 141.3, 137.6, 135.6, 132.4, 131.1, 129.9, 128.4, 124.7, 123.6, 119.2, 112.4, 56.7 ppm.

FT-IR: 1685 (C=O), 1649 (C=C), 1273 (C–N), 1105 (O-CH$_3$) cm^{-1}.

HRMS: 362.1137 (M+H$^+$) (Calculated for $C_{20}H_{16}N_3O_2$: 362.1161).

2.6.5 Procedure of dyeing (PET, Nylon, Acrylic)

PET, nylon and acrylic fabrics dyeing were performed on a Flexi Dyer dyeing machine with 1:30 MLR (material to liquor ratio) and percentage shade 2% (calculated on the weight of fabric). Firstly, the azo dye was pasted using dispersing agent Saragen-50 and further diluted using 15 ml of buffered solution with acetic acid in water (pH 4–5) [57]. Complete dispersion of the dye in water was acquired by ultra-sonication for 30 min. PET, NYL and ACR substrates dyed using above solutions. Dyeing was initiated at room temperature and raised to 130 °C (PET) and 90 °C (nylon), 90 °C (acrylic) respectively, maintain this raised temperature for 1 h and cool down to 60 °C. The dyed substrate thoroughly washed with warm and cold water and further for PET dyed fabric, reduction clearing treatment is given with 2gpl soda ash (Na$_2$CO$_3$), 1gpl soap solution and 2gpl Sodium hydrosulphite at 70 °C for 15 min, then treated fabric was washed with water and dried.

3 Results and discussion

3.1 Photo-physical properties

Dyes (**4a**–**4c**) showed dual absorption peaks while their corresponding methoxy derivatives (**5a**–**5c**) showed only single absorption peak (Fig. S2). Significant effect

of substituents (–Cl and –NO$_2$ group) was observed on absorption maxima of dyes (**4b** and **4c**) on comparing with unsubstitued dye (**4a**) in various solvents. But on comparing **4b** (–Cl) with **4c** (–NO$_2$), a very small difference was detected in the absorption maxima of the dyes. Only **4b** dye is slightly red shifted (1–3 nm) compared to **4c** in different solvents. Effect of –NO$_2$ and –Cl substituents on absorption spectra of the dyes are provided in the literature [58, 59]. The first absorption maxima of **4a**–**4c** corresponds to the azo form, while the second red shifted absorption maxima corresponds to the hydrazone form [60]. Methoxy group is better donating group as compared to the hydroxyl group and significant effect has been observed in absorption spectra. **5a**, **5b** and **5c** (exclusive azo forms) are absorbing at red shifted region as compared to corresponding azo form of hydroxyl derivatives **4a**, **4b** and **4c**, respectively. Additionally, distinct second absorption peak (red shifted) of hydrazone form at around 369–382 nm was observed for compounds **4a**, **4b** and **4c** which was disappeared in methoxy series (**5a**, **5b** and **5c**) due to the absence of hydrazone formation. Methoxy substituted parallel series (**5a**, **5b** and **5c**) showed similar trend solvatochromism as compared to their corresponding hydroxyl analogues (**4a**, **4b** and **4c**). The absorption maxima trend of dyes is as follows: **4a** < **4c** ≤ **4b** < **5a** ≤ **5b** < **5c** (Table 1). It is clearly observed that dyes **4a**, **4b** and **4c** has very good molar absorptivity as matched to methoxy analogues **5a**, **5b** and **5c**, respectively (Table 1).

3.2 Viscosity influenced spectroscopic characterization

Synthesized azo dyes are not emissive in solvents. The possible for non-radiative relaxation during de-excitation may be isomerizations and rotational motions through single bonds beside to azo group [61]. Substituent effects, solvent viscosity, solvent polarity and hydrogen bonding are also possible factors affects non-radiative rate [62–65]. So, viscosity helps to restrict rotations through the single bonds adjacent to azo. Azo-hydrazone tautomerism can also has contribution in restriction of the rotations in these dyes additionally. With the aim of consider polarity effects different polarity-viscosity binary mixtures (DMSO-Glycerol), (toluene-PEG400) and (toluene-paraffin oil) have been used. In this study we have chosen three different viscous binary mixtures i.e. DMSO-Glycerol (polar protic),toluene-PEG 400 (polar aprotic) and toluene–paraffin oil (non-polar aprotic). Quinine sulphate (in 0.5 M H$_2$SO$_4$, Φ_{fl} = 0.546) is used as a standard to calculate relative fluorescence quantum yield (Φ_{fl}).

Table 1 Photophysical properties of all dyes in various solvent

Dye	Toluene		Dioxane		CHCl$_3$		EtOAc		THF		MeOH		DMF		DMSO	
	λ_{max} (nm)	ε (mol^{-1}) (dm^3 cm^{-1})	λ_{max} (nm)	ε (mol^{-1}) (dm^3 cm^{-1})	λ_{max} (nm)	ε (mol^{-1}) (dm^3 cm^{-1})	λ_{max} (nm)	ε (mol^{-1}) (dm^3 cm^{-1})	λ_{max} (nm)	ε (mol^{-1}) (dm^3 cm^{-1})	λ_{max} (nm)	ε (mol^{-1}) (dm^3 cm^{-1})	λ_{max} (nm)	ε (mol^{-1}) (dm^3 cm^{-1})	λ_{max} (nm)	ε (mol^{-1}) (dm^3 cm^{-1})
4a	323	26,316	323	23,924	324	33,511	324	35,011	325	29,173	325	42,460	326	40,364	326	36,759
	372	14,950	370	13,529	372	18,619	370	19,787	373	17,034	370	23,996	369	22,848	371	20,217
4b	330	23,197	331	2577	331	27,671	331	19,275	331	20,016	332	18,014	332	21,949	332	24,219
	376	14,512	375	16,116	378	17,041	380	12,108	382	12,580	381	11,330	382	13,838	381	15,232
4c	329	22,238	330	23,408	330	19,897	331	16,386	331	17,556	331	18,493	332	20,904	332	16,514
	375	13,071	376	13,759	374	11,695	376	9631	375	10,319	376	10,869	376	12,286	377	9706
5a	346	15,261	346	12,717	347	13,903	348	12,933	349	10,777	350	13,547	351	10,669	351	11,855
5b	347	9272	348	8858	349	8993	349	10,303	350	10,986	351	11,857	352	8537	352	10,671
5c	362	3457	362	3142	363	3457	364	4148	364	2828	365	3771	366	3079	367	2514

λ_{max}: Absorption maximum wavelength, ε: Molar extinction coefficient

3.2.1 DMSO- glycerol mixture

(a) *Spectral data*

Absorption maxima of dyes were documented in varying extremely viscous medium Glycerol-DMSO at constant concentration (Fig. 1). Dyes (**4a**–**4c**) exhibited broad and dual absorption peaks (azo form and hydrazone form) while only single absorption peak with slight red shift was observed for the corresponding methoxy derivatives (**5a**–**5c**) (Fig. 1).

Azo forms of dyes (**4aA**, **4bA** and **4cA**) did not exhibit noteworthy emission intensity progressing Glycerol-DMSO mixtures (Fig. 2). Calculated relative fluorescence quantum yields and fold of increase and at Glycerol(9.5):DMSO(0.5) v/v compared to blank DMSO for the dyes are 8.8 fold($\Phi_{fl} = 4\%$) for **4aA**, 8.3 fold($\Phi_{fl} = 5\%$)for **4bA** and 6.3 fold ($\Phi_{fl} = 3\%$) for **4cA**. Similar trends were observed for the corresponding methoxy analogues, i.e. **5a** showed 17.5 fold ($\Phi_{fl} = 3\%$), **5b** showed 15.7 fold ($\Phi_{fl} = 3\%$) and **5c** showed 12.5fold ($\Phi_{fl} = 4\%$) at Glycerol (9.5): DMSO(0.5) v/v binary mixture (Fig. 2). On the other hand, hydrazone form of dyes **4aH, 4bH and 4cH** in Glycerol-DMSO binary mixture exhibited significant emission intensity enhancement with increasing Glycerol content. Hydrazone forms **4aH** showed 96 fold ($\Phi_{fl} = 30\%$), **4bH** showed 78 fold ($\Phi_{fl} = 27\%$) and **4cH** showed 75 fold ($\Phi_{fl} = 29\%$) at Glycerol (9.5):DMSO (0.5) v/v (Fig. 2).
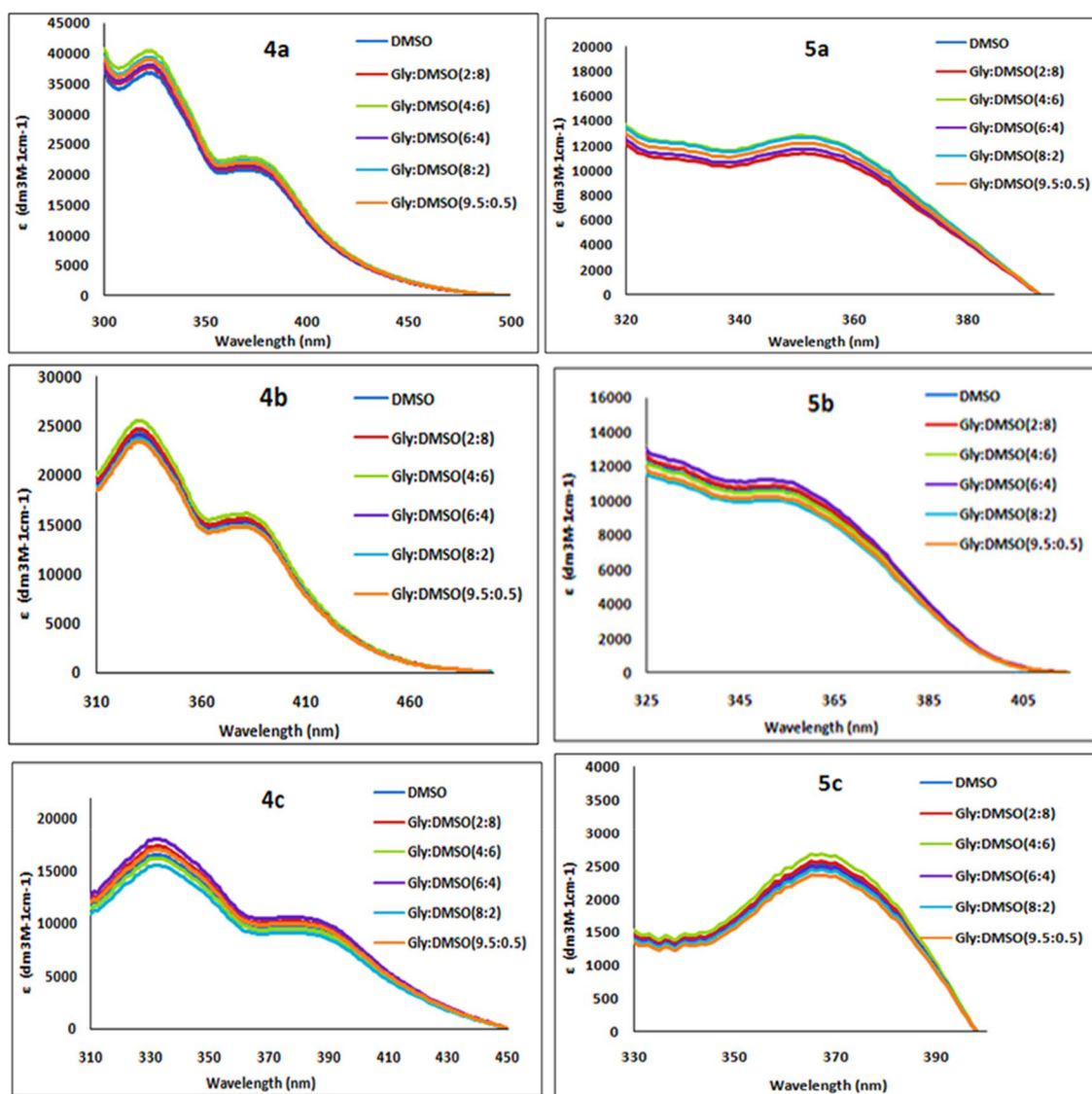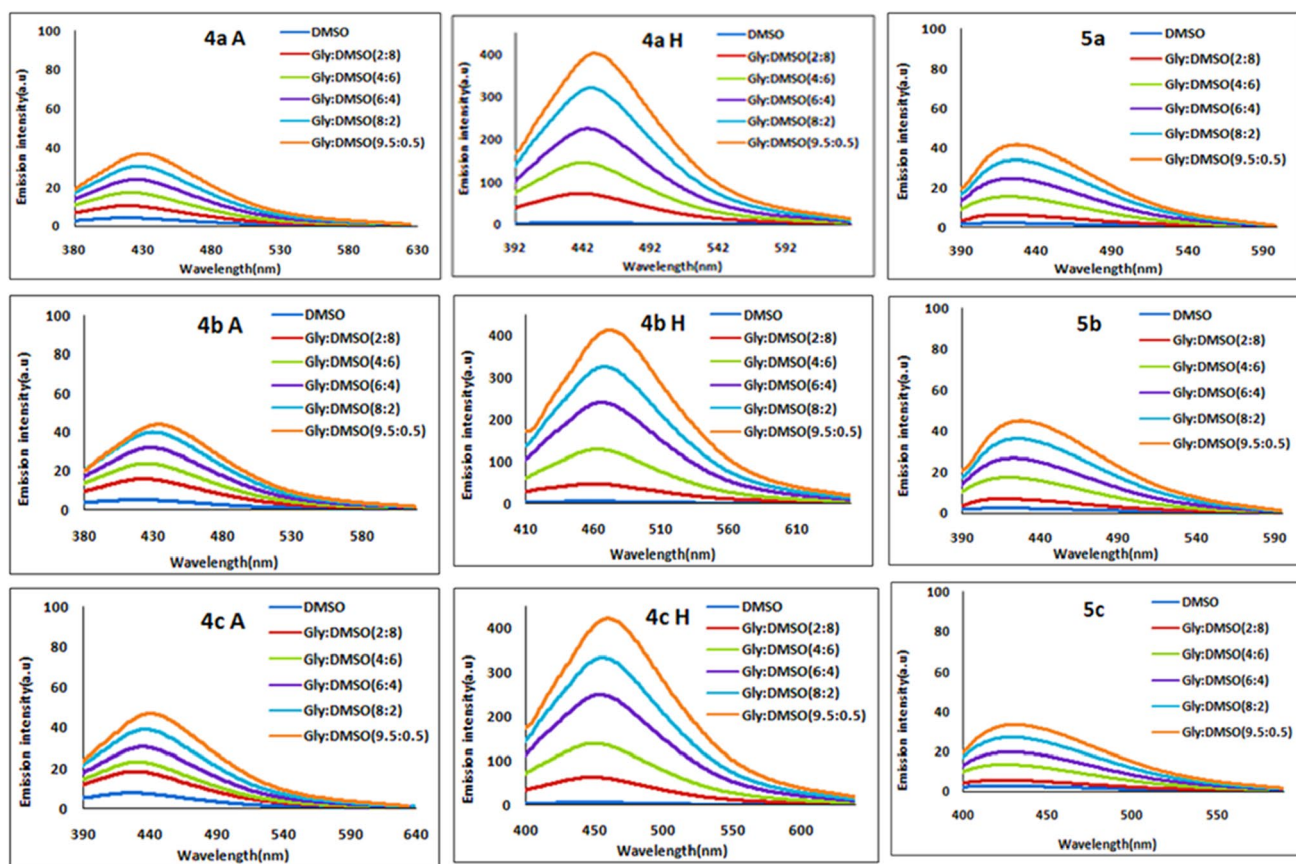

Fig. 1 Absorption spectra of **4a**, **4b**, **4c** and **5a**, **5b**, **5c** dyes in DMSO–Glycerol mixture ratio

Fig. 2 Emission spectra of **4aA** (excited @ 326 nm), **4bA** (excited @ 333 nm) and **4cA** (excited @ 332 nm), **5a** (excited @ 351 nm), **5b** (excited @ 365 nm), **5c**(excited @ 367 nm), **4aH** (excited @ 372 nm), **4bH** (excited @ 384 nm) and **4cH** (excited @ 381 nm) in DMSO–Glycerol mixture ratio

This result suggest hydrogen bonding involved in azo-hydrazone tautomerizm along with viscosity has a significant part in emission enhancement. Methoxy analogues of these dyes **5a**, **5b** and **5c** did not show significant emission intensity enhancement may be due to absence of hydrogen bonding center. Alternately, this can be explained and supported by more planarity attainment of hydrazone forms than the corresponding azo-methoxy forms of the dyes in viscous environment. Hence, both azo form and methoxy forms are less emissive as compared to hydrazone forms of the dyes.

(b) *Viscosity sensitivity result*

Forster-Hoffman equation is used to quantify viscosity sensitivity of synthesized azo dyes

$$\text{Log } I = C + x \text{ log} \qquad (2)$$

Where,

η = viscosity (mPa s).

X = viscosity sensitivity parameter,

I = maximum emission intensity and.

C = constant.

Viscosity sensitivity against emission intensity plotted. Viscosity rises from 1.99 mPa s (DMSO) to 688.51 mPa s for (DMSO:Gly: 5:95).It is clearly observed that all the hydrazone forms of the dyes have significant viscosity sensitivity **4aH(x = 0.676)**, **4bH (x = 0.690)** and **4cH(x = 0.673)** with good regression coefficients on excitation @ 370–381 nm (Fig. 3). On the other hand azo forms **4aA, 4bA and 4cA** have exhibited viscosity sensitivity **(x) 0.349, 0.337 and 0.292**, respectively. Similarly, methoxy analogues **5a, 5b and 5c** have exhibited viscosity sensitivity **(x) 0.499, 0.456 and 0.470**, respectively. Comparative viscosity trend for all the dyes is found to be **4bH ≥ 4 aH ≥ 4cH > 5a ≥ 5c ≥ 5b > 4aA ≥ 4bA ≥ 4cA** (Fig. 3).

(c) *Viscosity polarity effect*

As polarity of viscous media increases not only emission intensity enhancement but also red shifting in emission wavelength has been observed. Therefore, we have related solvent polarity functions with stokes shift and emission wavelength of dyes. For this purpose Lippert-Mataga and Weller equa-
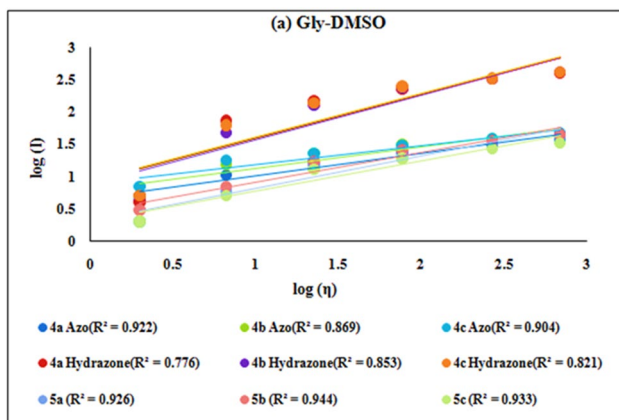
Fig. 3 Comparative viscosity against intensity (logarithmic) spectrum of dyes in different DMSO-Glycerol mixture ratio

tion has been used and solvatochromic behavior of synthesized dyes estimated. Lippert-Mataga plot indicated that azo forms of the dyes **4aA, 4bA and 4cA** exhibited large Stokes shifts **6646–7649 cm^{-1}** and positive solvatochromism (Fig. 4). On the other hand small Stokes shifts and positive solvatochromism were observed for corresponding methoxy analogues **5a, 5b and 5c (3828–5126 cm^{-1})**. Similarly, hydrazone forms of the dyes showed small Stokes shift and positive solvatochromism **(4053–5015 cm^{-1})** and are in good correlation to fluorescence quantum yields.

Maximum Stokes shifts were observed for **4a–4c** and found to have very good correlation of having low fluorescence quantum yields. Weller plot showed that azo forms of the dyes **(4aA, 4bA and 4cA)** exhibited emission wavelengths 16,000–23,980 cm^{-1}. Similar trend was observed for the corresponding methoxy analogues **5a, 5b and 5c** (23,255–24,154 cm^{-1}). On the other hand hydrazone forms of the dyes

showed longest emission wavelengths (21,231–22,831 cm^{-1}) among all dyes. Hydrazone forms of dyes show more red shifting emission and lowest Stokes shifts as compared to corresponding azo and methoxy forms of dyes and are in a good agreement with quantum yields. Positive solvatochromism observed for all the dyes presented in (Fig. 4).

3.2.2 Toluene-PEG 400 mixture

(a) *Spectral data*

Absorption spectra of (**4a**–**4c**) and (**5a**–**5c**) dyes having same concentration were recorded in varying toluene-PEG400 mixture ratio. Dyes (**4a**–**4c**) showed dual and broad absorption peaks (azo form and hydrazone form) while only single absorption peak with slight red shift was observed for the corresponding methoxy derivatives (**5a**–**5c**) (Fig. S3). Azo forms of dyes (**4aA**, **4bA** and **4cA**) did not exhibit significant emission intensity enhancement in varying ratio of toluene-PEG400 binary mixture (Fig. 5). Calculated relative fluorescence quantum yields and fold of increase at toluene(0.5):PEG400(9.5) v/v compared to toluene for the dyes are 8.6 fold ($\Phi_{fl}=3\%$) for **4aA**, 7.6 fold ($\Phi_{fl}=4\%$) for **4bA** and 7 fold ($\Phi_{fl}=3\%$) for **4cA**. Similar trends were observed for methoxy analogues, i.e. **5a** showed 7 fold ($\Phi_{fl}=2\%$), **5b** showed 6.5 fold ($\Phi_{fl}=3\%$) and **5c** showed 7.3 fold ($\Phi_{fl}=4\%$) at toluene-PEG400 0.5:9.5 (v/v) binary mixture. On the other hand, hydrazone form of dyes **4aH, 4bH and 4cH** in toluene-PEG400 binary mixture exhibited significant emission intensity enhancement with increasing PEG 400 content. Hydrazone forms **4aH** showed 47.5 fold ($\Phi_{fl}=24\%$), **4bH** showed 55.6
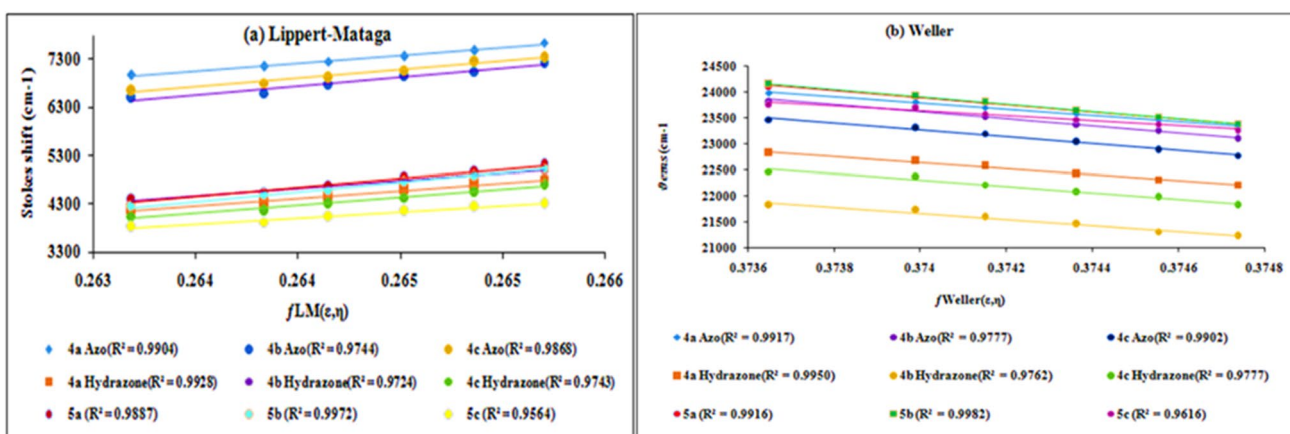
Fig. 4 Weller and Lippert-Mataga plots in different DMSO-Glycerol mixture ratio
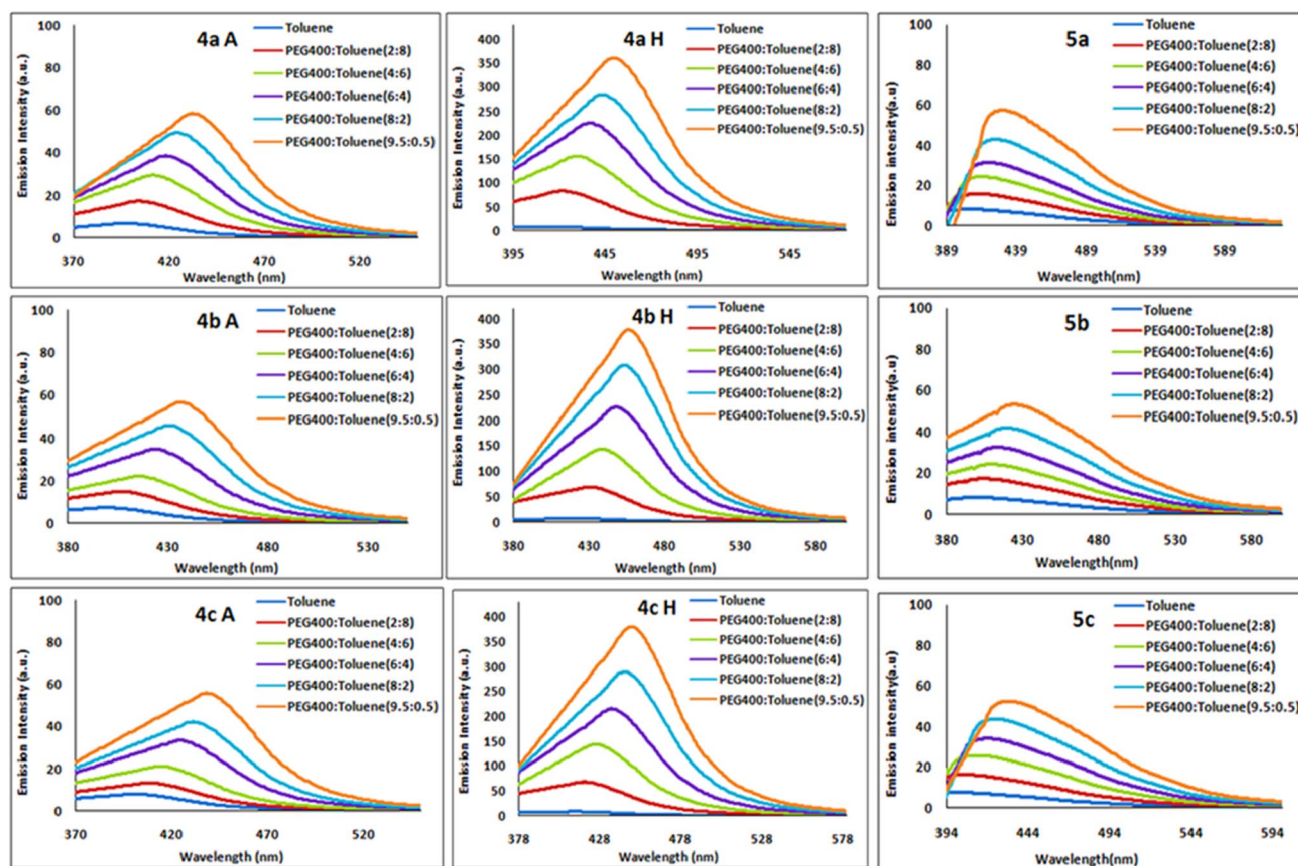
Fig. 5 Emission spectra of **4aA** (excited @ 323–327 nm), **4bA** (excited @ 329–333 nm) and **4cA** (excited @ 328–332 nm), **5a** (excited @ 346–349 nm), **5b** (excited @ 361–364 nm) and **5c** (excited @ 362–365 nm), **4aH** (excited @ 369–373 nm), **4bH** (excited @ 380–383 nm) and **4cH** (excited @ 377–380 nm) in various toluene-PEG400 mixture ratio

fold (Φ_{fl} = 22%) and **4cH** showed 47.5 fold (Φ_{fl} = 25%) at toluene-PEG400 (0.5:9.5 v/v) (Fig. 5). In toluene-PEG 400 mixture polarity is changing drastically as compared to DMSO-Glycerol mixture, but hydrazone forms of the dyes **(4aH, 4bH and 4cH)** showed similar emission enhancement in both the viscous medium.

(b) *Viscosity sensitivity effect*

In toluene-PEG400binary mixtures viscosity increases from 0.55 mPa s (toluene) to 42.21 mPa s (toluene: PEG400: 5:95). Hydrazone forms of the dyes showed excellent viscosity sensitivity **4aH(X=0.646), 4bH(x=0.697) and 4cH(x=0.675)** with moderately good regression coefficients on excitation @ **372–378 nm** (Fig. 6). On the other hand azo forms **4aA, 4bA and 4cA** have exhibited viscosity sensitivity **(x) 0.407, 0.417 and 0.413** respectively. Similarly, methoxy analogues **5a, 5b and 5c** have exhibited viscosity sensitivity **(x) 0.399, 0.366 and 0.387** respectively. Comparative viscosity trend for all the dyes is found to be **4bH ≥ 4cH ≥ 4aH > 4bA ≥ 4cA ≥ 4aA > 5a ≥ 5c ≥ 5b**.
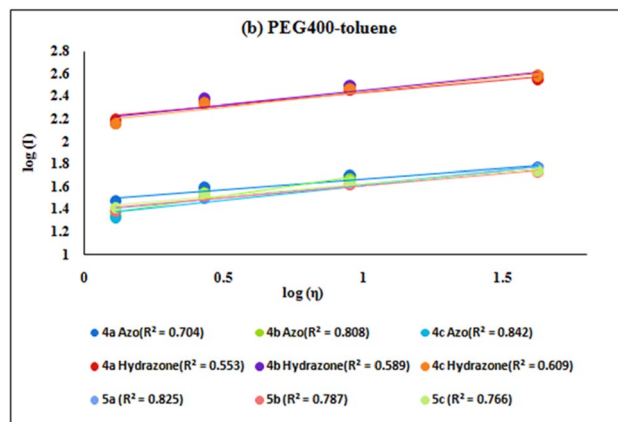
Fig. 6 Comparative viscosity against intensity (logarithmic) spectrum of dyes in differenttoluene-PEG400 mixture ratio

(c) *Viscosity polarity effect*

Lippert-Mataga plot showed that azo forms of the dyes **4aA**, **4bA** and **4cA** exhibited positive solvatochromism and large Stokes shifts 5148 cm^{-1} to

7246 cm^{-1} (Fig. 7). On the other hand small Stokes shifts and positive solvatochromism were observed for corresponding methoxy analogues **5a, 5b and 5c (2498–5343 cm^{-1}).** Similarly, hydrazone forms of the dyes showed small Stokes shift and positive solvatochromism **(2668–4810 cm^{-1})** and are in good correlation to fluorescence quantum yields. Maximum Stokes shifts were observed for **4aA–4cA** and found to have very good correlation of having low fluorescence quantum yields. Weller plot showed that azo forms of the dyes **(4aA, 4bA and 4cA)** exhibited emission wavelengths **22,831–25,188 cm^{-1}**. Similar trend was observed for corresponding methoxy analogues **5a, 5b and 5c (23,148–25,125 cm^{-1})**. On the other hand hydrazone forms of the dyes showed longest emission wavelengths **(21,645–24,213 cm^{-1})** among all dyes. Hydrazone forms of dyes exhibited more red shifted emissions and lowest Stokes shifts paralleled to analogous azo and methoxy dyes. Positive solvatochromism has been observed in all the dyes as shown in Fig. 7.

3.2.3 Toluene–paraffin oil mixture

(a) *Spectral data*

Absorption spectra of dyes in varying toluene–paraffin oil (non-polar viscous medium) were recorded at constant concentration. Dyes (**4a**–**4c**) showed dual and broad absorption peaks (azo form and hydrazone form) while only single absorption peak with slight red shift was observed for the corresponding methoxy derivatives (**5a**–**5c**) (Fig. S4). Azo forms of dyes (**4aA**, **4bA** and **4cA**) did not showed noticeable emission intensity enhancement in varying ratio of toluene-parafin oil binary mixture **(**Fig. 8). Calculated relative fluorescence quantum yields and fold of increase at toluene(0.5):parafin oil(9.5) *v/v*in comparison with blank toluene for the azo forms of dyes **4aA, 4bA and 4cA** are7.9 fold (Φ_{fl} = 3%), 6.7fold (Φ_{fl} = 5%)and 7.3fold (Φ_{fl} = 4%) respectively at toluene-parafin oil0.5:9.5 (v/v) (Fig. 8). Methoxy analogues, i.e. **5a** showed 6.5fold (Φ_{fl} = 3%), **5b** showed 7.5 fold (Φ_{fl} = 4%) and **5c** showed 6.6 fold (Φ_{fl} = 5%) increase at toluene–paraffin oil at 0.5:9.5 (v/v) binary mixture compared to toluene. On the other hand, hydrazone forms **4aH** showed 50.5 fold (Φ_{fl} = 27%), **4bH** showed 58.9 fold (Φ_{fl} = 26%) and **4cH** showed 52.1 fold (Φ_{fl} = 28%) at toluen-paraffin oil 0.5:9.5 (v/v) (Fig. 8). In non-polar viscous mixture also hydrazone forms have found viscosity influenced emission enhancements compared to their respective azo and methoxy forms confirms that hydrogen bonding along with the viscosity played an important role in the emission.

(b) *Viscosity sensitivity effect*

In toluene-paraffin oil binary mixture viscosity increases from 0.55 mPa s (toluene) to 220.93 mPa s (toluene:paraffin: 5:95). The hydrazone forms of the dyes show high viscosity sensitivity and are found to be **4aH (x = 0.448), 4bH (x = 0.479) and 4cH (x = 0.458)**with regression coefficients on excitation **@ 372–378 nm**. On the other hand azo forms **4aA, 4bA and 4cA** have exhibited viscosity sensitivity **(x) 0.294, 0.264 and 0.269** respectively. Similarly, methoxy analogues **5a, 5b and 5c** have exhibited viscosity sensitivity **(x) 0.252, 0.270 and 0.256** respectively. Comparative viscosity trend for all the dyes is found to be in the order **4bH ≥ 4cH ≥ 4aH > 4aA ≥ 5b ≥ 4cA > 4bA > 5c ≥ 5a** (Fig. 9).

(c) *Viscosity polarity effect*

Lippert-Mataga plot showed that azo forms of the dyes **4aA, 4bA and 4cA** showed positive solvatochromism and large Stokes shifts from **4841 to**
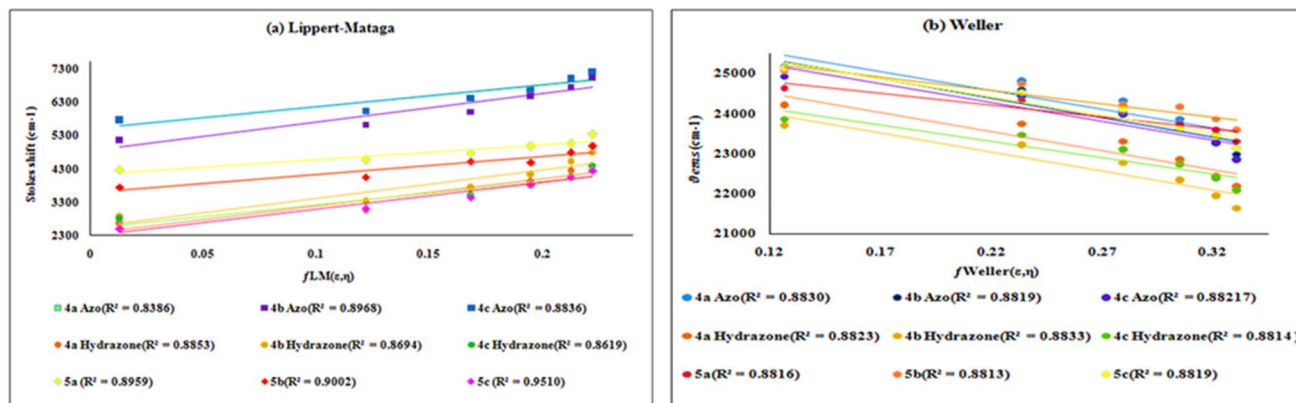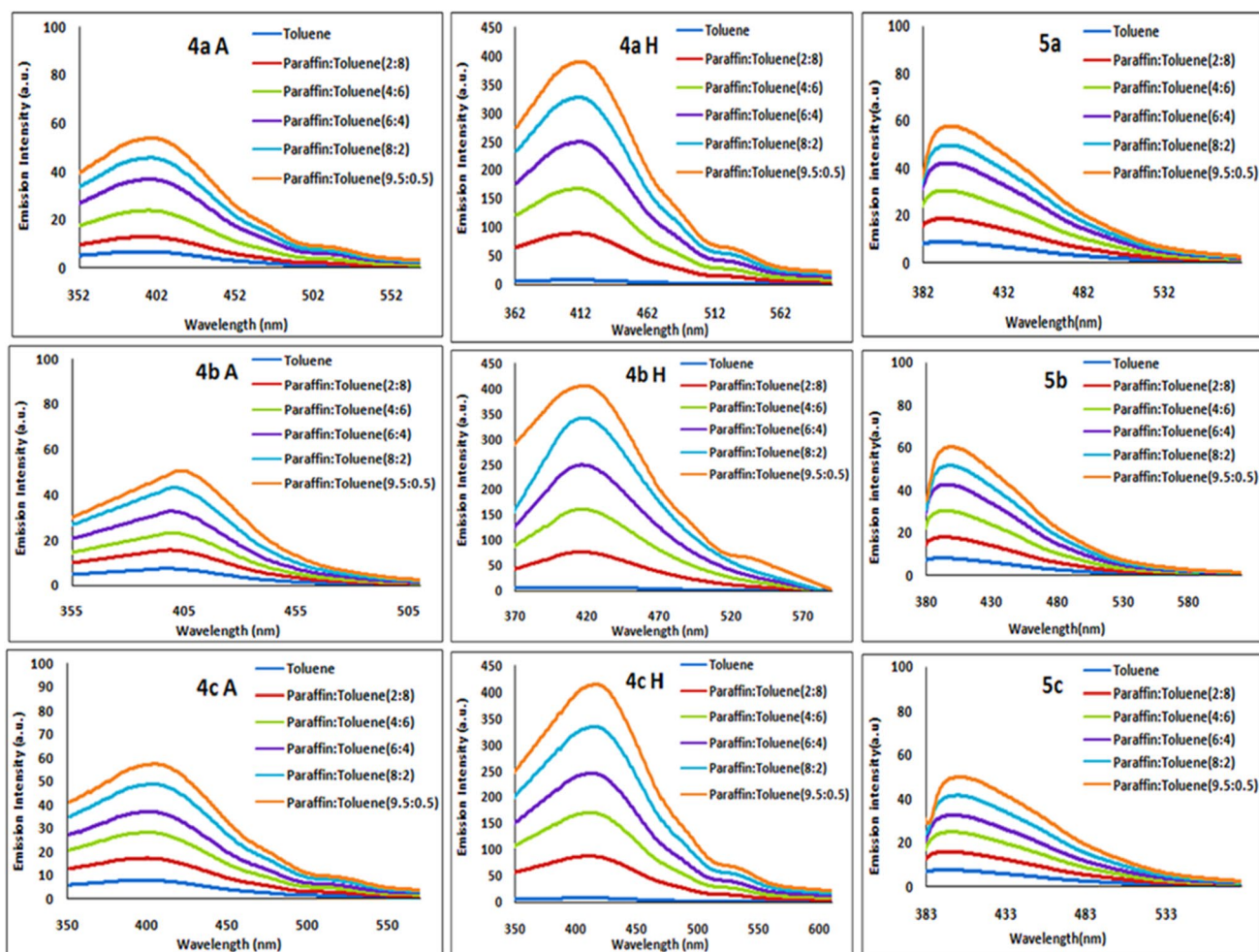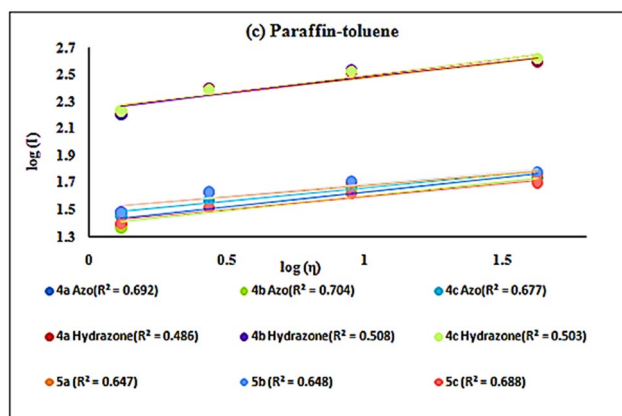

Fig. 7 Lippert-Mataga and Weller plots in toluene-PEG400 mixture ratio

Fig. 8 Emission spectra of **4aA** (excited @ 323 nm), **4bA** (excited @ 329 nm) and **4cA** (excited @ 328 nm), **5a** (excited @ 346 nm), **5b** (excited @ 361 nm) and **5c** (excited @ 362 nm), **4aH** (excited @ 369 nm), **4bH** (excited @ 380 nm) and **4cH** (excited @ 377 nm) in various toluene–paraffin oil mixture ratio

Fig. 9 Comparative viscosity against intensity (logarithmic) spectrum of dyes in different toluene–paraffin oil mixture ratio

5612 cm^{-1} (Fig. 10). On the other hand small Stokes shifts and positive solvatochromism were observed for corresponding methoxy analogues **5a, 5b and 5c** (**2307–3755 cm^{-1}**). Similarly, hydrazone forms of the dyes showed small Stokes shift and positive solvatochromism (**2335–2609 cm^{-1}**) and is in good correlation to fluorescence quantum yields. Maximum Stokes shifts were observed for **5a–5c**. Azo dye and found to have very good correlation of having low fluorescence quantum yields. Weller plot showed that azo forms of the dyes (**4aA, 4bA and 4cA**) exhibited emission wavelengths in between **24,691 and 25,316 cm^{-1}**. Similar trend was observed for corresponding methoxy analogues **5a, 5b and 5c** (**24,813–25,380 cm^{-1}**). On the other hand hydrazone forms of the dyes showed emission wavelengths (**23,866–24,509 cm^{-1}**) among all dyes. Hydrazone forms of dyes showed red shifting emissions and low-
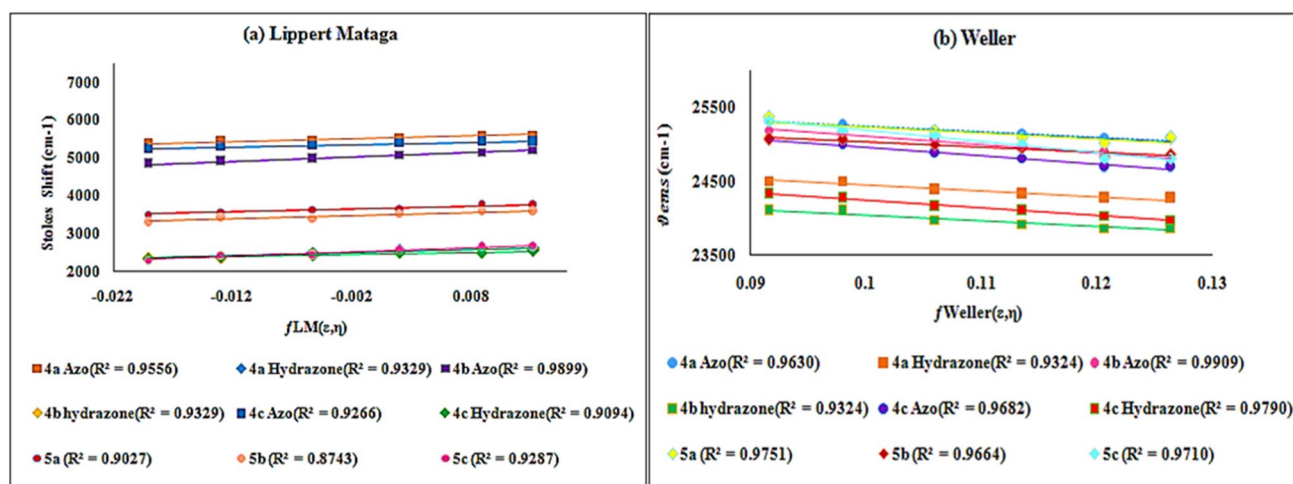
Fig. 10 Lippert-Mataga and Weller plots in toluene–paraffin oil mixture ratio

est Stokes shifts related to analogous azo and methoxy forms and are in good agreement with quantum yields. Positive solvatochromism has been observed for all as shown in Fig. 10.

In summary hydrazone forms of dyes **(4aH–4cH)** have shown maximum and significant enhancement in emission intensity as compared to azo forms of dyes **(4aA–4cA)** and parallel methoxy derivatives **(5a–5c)** in varying polarity viscous mixtures i.e. DMSO-Glycerol (polar protic), toluene-PEG 400 (mid polar) and toluene–paraffin oil (nonpolar aprotic). This suggested that viscosity and hydrogen bonding (involved in aza-hydrazone tautomerism) are playing crucial role in the enhancement while polarity of the viscous mixture has a significant role in bathochromic shift in the absorption maxima and emission wavelength. We observed good correlation of Stokes shifts ($\Delta \bar{\upsilon}$) and fluorescence quantum yields (Φ_f) of all dyes in the viscous mixture. Hydrazone forms may be attaining more planarity due to hydrogen bonding along with viscosity.

3.3 Spectral characteristics

Influence of viscosity and its variable polarity of three viscous binary mixtures on spectral characteristics of dyes has been assessed. It has been identified that with increasing viscous Glycerol, PEG 400 and paraffin oil medium in non-viscous DMSO and toluene medium caused increase in quantum yield (Φ_{fl}), radiative rate constant (K_r) and life time(τ) (Table 2).

All the dyes exhibited positive solvatochromism. Hydrazone forms showed highest fluorescence quantum yields and small Stokes shifts than corresponding azo and

methoxy analogues in all the viscous mixtures and are in a good agreement with the radiative rate constant (K_r). Non-radiative rate constant (K_{nr}) decreases with the increasing viscosity. $K_{nr} >> K_r$ clearly indicates that these azo dyes de-excited favorably in non-radiative manner even in the viscous medium (Table 2). Estimated spectral characteristics at the lowest and the highest viscous media of three binary mixtures are presented in Table 2.

3.4 Aggregation induced emission enhancement

Aggregation induced emission enhancement study carried out for synthesized azo dyes with different H_2O fractions in THF. Dyes (**4a**–**4c**) showed two absorptions in the range of 325,331,331 nm and second absorption at 373, 382,375 nm respectively. Excitation at shorter wavelength did not exhibit any AIEE characteristics for (**4a–4c**) dyes but, at longer wavelength the dyes exhibited steady change in emission intensity. In THF and THF/H_2O mixtures with different H_2O fractions lower than 50% dyes exhibited weak fluorescence and fluorescence increased with water fractions from 60 to 90% in THF/H_2O mixture (Fig. 11 and Fig. S2). We noticed that emission intensity also increased at concentration from 20 to 40% in THF/H_2O mixture but compared to the 50% THF/H_2O mixture the emission intensity observed was less. This emission intensity enhancement could be attributed to the restricted rotation of N=N bond in solvent-water mixture prominent to formation of molecular aggregates.

3.5 Color co-ordinates

K/S values of dyes estimated using equation [66].

Table 2 Estimated photophysical properties of all dyes in varies viscous mixtures

Dye	Entry	DMSO	DMSO:Glycerol (0.5:9.5 v/v)	Toluene	Toluene:PEG400 (0.5:9.5 v/v)	Toluene	Toluene:paraffinoil (0.5:9.5 v/v)
4aA	Φ_f	0.44	4	0.34	3	0.37	3
	τ (ns)	0.01	0.03	0.02	0.05	0.01	0.05
	Kr (s^{-1}) ($\times 10^8$)	1.4	2.1	2.3	2.7	1.9	2.5
	K_{nr} (s^{-1}) ($\times 10^{10}$)	62.4	3.2	78.3	2.1	80	1.8
4aH	Φ_f	0.31	30	0.50	24	0.53	27
	τ (ns)	0.01	0.07	0.02	0.08	0.01	0.06
	Kr (s^{-1}) ($\times 10^8$)	2.2	3.8	2	3.6	1.8	2.9
	K_{nr} (s^{-1}) ($\times 10^{10}$)	73.7	0.32	80.6	0.21	59.2	0.11
5a	Φ_f	0.17	3	0.28	2	0.46	3
	τ (ns)	0.01	0.06	0.02	0.04	0.01	0.03
	Kr (s^{-1}) ($\times 10^8$)	7.7	10.5	3.6	5.7	6.3	8.3
	K_{nr} (s^{-1}) ($\times 10^{10}$)	4.8	1.7	5.2	1.5	4.3	2.1
4bA	Φ_f	0.6	5	0.52	4	0.74	5
	τ (ns)	0.02	0.05	0.01	0.04	0.02	0.06
	Kr (s^{-1}) ($\times 10^8$)	3.3	5.2	2.9	4.1	2.7	3.5
	K_{nr} (s^{-1}) ($\times 10^{10}$)	8.2	1.3	7.4	2.3	5.8	1.7
4bH	Φ_f	0.34	27	0.39	22	0.44	26
	τ (ns)	0.01	0.07	0.01	0.06	0.02	0.08
	Kr (s^{-1}) ($\times 10^8$)	3.1	4.3	2.2	3.8	2.8	4.1
	K_{nr} (s^{-1}) ($\times 10^{10}$)	62.4	0.28	58	0.13	71.3	0.12
5b	Φ_f	0.19	3	0.46	3	0.53	4
	τ (ns)	0.01	0.04	0.02	0.05	0.01	0.03
	Kr (s^{-1}) ($\times 10^8$)	7.2	10.2	3.5	9.2	8.3	13.2
	K_{nr} (s^{-1}) ($\times 10^{10}$)	11.4	1.8	13.5	1.2	17.8	1.1
4cA	Φ_f	0.5	3	0.42	3	0.54	4
	τ (ns)	0.01	0.04	0.01	0.05	0.02	0.05
	Kr (s^{-1}) ($\times 10^8$)	5.2	5.9	4.8	5.4	6.1	6.5
	K_{nr} (s^{-1}) ($\times 10^{10}$)	14.2	0.8	9.8	1.3	7.3	0.9
4cH	Φ_f	0.38	29	0.52	25	0.53	28
	τ (ns)	0.02	0.06	0.02	0.08	0.01	0.07
	Kr (s^{-1}) ($\times 10^8$)	6.3	6.8	5.9	6.7	5.2	6.1
	K_{nr} (s^{-1}) ($\times 10^{10}$)	48.3	0.3	53.7	0.43	68.4	0.3
5c	Φ_f	0.32	4	0.54	4	0.75	5
	τ (ns)	0.01	0.05	0.02	0.07	0.01	0.06
	Kr (s^{-1}) ($\times 10^8$)	7.2	7.8	6.9	7.5	6.7	7.1
	K_{nr} (s^{-1}) ($\times 10^{10}$)	15.3	2.2	17.4	1.2	11.2	1.1

$$K/S = \frac{(1-R)^2}{2R}$$

Where,

R = reflectance

K and S = absorption and scattering coefficients, respectively.

Synthesized disperse azo dyes applied on PET, NYL and ACR fabric at 2% shade, 1:30 MLR (Material to liquor ratio). The CIELAB system (L^*, a^* and b^*) used for evaluation of dyed substrate. Dyes on applying to PET dyeing showed that hue (h0) of methylated form is less than compare to hydroxyl form of benzophenone based azo dyes. **4a** show highest hue (yellowish) and **4c** show lowest hue (Reddish) (Table 3a). Table 3b showed color coordinates of nylon dyeing where no specific observation observed. All the dyes show hues (h^0) in between 77.25–89.26 (Yellowish) but K/S values of hydroxyl dyes (**4a, 4b, 4c**) is slightly greater than methylated dyes (**5a, 5b, 5c**). Dyes on applying to acrylic dyeing showed similar observations as that on nylon (Table 3c).
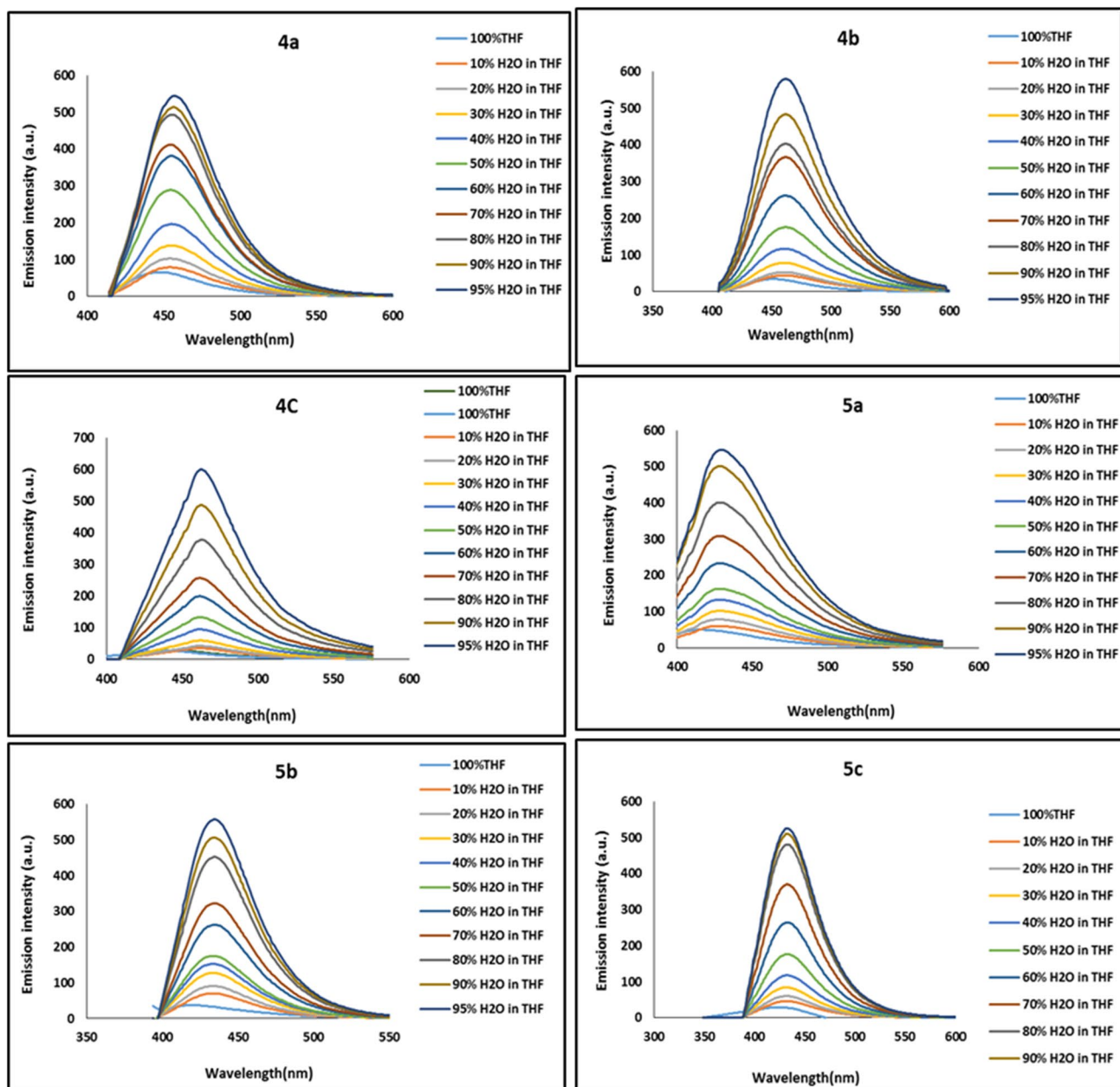
Fig. 11 Emission spectra of **4a**, **4b**, **4c** and **5a**, **5b**, **5c** dyes in THF–H$_2$O mixtures with different water fractions (5 μM)

Table 3a Color coordinates (CIELAB) for PET dyeing

Dye	L*	a*	b*	c*	h^0	K/S
4a	73.1	9.5	73.8	74.4	82.6	25.73
4b	65.5	14.4	68.6	70.1	78.1	17.28
4c	63.3	17.9	68.4	70.7	75.3	24.73
5a	50.3	21.3	57.7	61.5	69.7	2.28
5b	47.7	21.7	53.8	58.1	68.0	2.26
5c	53.4	23.3	49.5	54.7	64.7	10.05

On the other hand, dyes bond strongly to PET and are slightly affected by UV radiations [67, 68]. Hence, PET is more suitable than nylon for the dyes under investigations.

3.5.1 Fastness properties

After heat setting at 180 °C for 60 s the dyed substrates were tested in a sublimation testing machine at 177 °C for 30 s. The tested fabrics were rated against the standard Grey scales (1–5 grade) where 1 is poor and 5 is excellent grade for sublimation fastness. Sublimation fastness test result values range from moderate to excellent (Table 4). On comparison between all dyed fabrics PET samples show little better sublimation fastness than acrylic and nylon dyed fabric. The sublimation fastness results in (Table 4) observed that the dyes containing substituent groups such as $-NO_2$, $-Cl$ (**4b**, **4c**, **5b**, **5c**) has better

sublimation fastness than unsubstitued (**4a**, **5a**) dyes. Substituted group tend to increase the and hence their sublimation fastness were increased [69]

Comparative light fastness of hydroxyl dyes and corresponding methylated forms of these benzophenone based azo dyes has performed to get insight into role of H-bonding and methylation simultaneously. From Table 4 it is observed that light fastness of all the dyes varies from very good to excellent. On PET fabric dyes show excellent light fastness. On nylon fabric dyes show very good to excellent light fastness. On acrylic fabric dyes show less light fastness rating as compared to PET and nylon.

It is well known that nitro-substituted dyes give poor light fastness on nylon but, in our case dye **4c** and **5c** exhibited very high photostability on nylon. Most commercial disperse dyes are aniline or N,N-dialkylaniline substituted. On such dyes some light fastness—structure

Table 3b Color coordinates (CIELAB) for nylon dyeing

Dye	L*	a*	b*	c*	h^0	K/S
4a	69.4	7.9	54.4	55.0	81.7	7.89
4b	68.8	0.6	47.9	47.9	89.3	3.75
4c	65.1	10.5	46.4	47.5	77.3	8.06
5a	53.8	3.8	28.8	29.1	82.4	1.10
5b	59.1	6.5	35.1	35.7	79.4	1.85
5c	66.4	4.4	46.5	46.7	84.5	2.75

Table 3c Color coordinates (CIELAB) for acrylic dyeing

Dye	L*	a*	b*	c*	h^0	K/S
4a	57.9	13.4	48.2	50.0	74.5	14.05
4b	61.1	7.1	46.9	47.5	81.4	10.34
4c	60.8	12.5	49.9	51.5	75.9	14.52
5a	53.1	13.1	46.1	47.9	74.1	5.40
5b	44.0	7.1	31.1	31.9	77.0	2.34
5c	51.3	16.0	39.3	42.4	67.8	6.85

Table 4 Light and sublimation fastness ratings for dyed PET, nylon and acrylic samples

Dye	PET		Nylon		Acrylic	
	Light	Sublimation	Light	Sublimation	Light	Sublimation
	Fastness rating	Fastness rating	Fastness rating	Fastness rating	Fastness rating	Fastness rating
	(1–8)*	(1–5)*	(1–8)*	(1–5)*	(1–8)*	(1–5)*
4a	8	4/5	7/8	4	7	3/4
4b	8	5	8	5	7/8	4
4c	8	5	8	4/5	6/7	4
5a	8	4/5	7/8	4	7	3
5b	8	5	7/8	4/5	7	4
5c	8	5	8	5	7	4

Rating* (Light fastness: 1-poor and 8-Excellent) (Sublimation Fastness: 1-poor and 5-Excellent)

correlations indicate that the fastness increases as the substituent in the para position is made more electronegative [70] and second substituent in the ortho position have a profound effect on light fastness. Light fastness increases with increasing electron-donating power of the ortho substituents to the azo linkage [71]. The dye **4c** and **5c** is an identical example for this criteria (Scheme 1). Therefore, *p*-nitro dye (**4c** and **5c**) being most light fast on nylon.

Comparative light and sublimation fastness of present benzophenone based disperse azo dyes and previously reported disperse azo dyes are tabulated in Table 5. Both hydroxyl and methylated forms of benzophenone based azo dyes show much better sublimation and light fastness as compared to the earlier reported dyes (Table 5).

3.5.2 Percentage exhaustion determination

The % exhaustion of dye bath achieved by collecting sample before and after dyeing. Optical density of each sample were recorded using UV–Vis spectrometer (Perkin Elmer Lambda 25 at λ_{max}) of the corresponding dye to get concentration of dye (g/l). The % exhaustion (E%) of dyes on PET, nylon and acrylic fabrics was calculated using equation [72].

$$\%Exhaustion = \frac{Initial\ OD_0 - Final\ OD_1}{Iniltial\ OD_0} \times 100 \qquad (3)$$

Where,
OD = optical density.
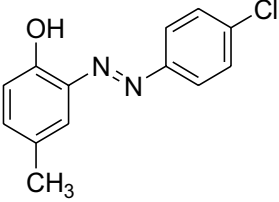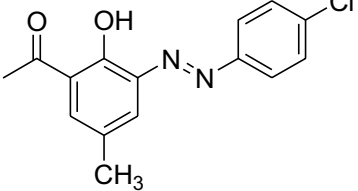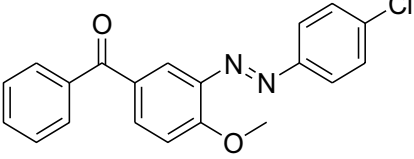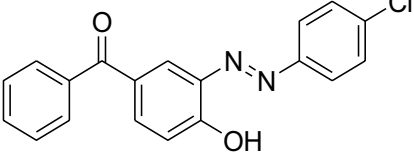OD_0 = optical density before the start of dyeing.
OD_1 = optical density at the end of dyeing.
Table 6 represents percentage exhaustion of dyes. All dyes showed exhaustion better on PET, nylon than acrylic substrate.

3.5.3 Ultraviolet protection factor

Ultraviolet protection factor (UPF) is the term used to quantify the amount of ultraviolet (UV) protection provided to skin by fabric [73]. Ultra-Protection Factor

Table 5 Comparison of light fastness and sublimation fastness with previous published work

Sr. no.	Structure	PET		Nylon		Reference
		Light fastness	Sublimation fastness	Light fastness	Sublimation fastness	
1		6	3	4	3	[74]
2		7	3	5	4	[15]
3		8	5	7	4	This work
4		8	5	8	5	This work

Table 6 Percentage exhaustion and fixation of all dyes on PET, nylon, acrylic

Dyes no.	PET (%)	Nylon (%)	Acrylic (%)
	Exhaustion	Exhaustion	Exhaustion
4a	83	80	45
4b	98	87	50
4c	77	75	42
5a	91	88	54
5b	96	70	44
5c	82	72	41

(UPF), UV-A blocking [400–320 nm] and UV-B blocking [320–280 nm] were tested to check the UV stability of dyed substrate. UVA range has major effects on skin such as wrinkles, drying, discoloration, skin cornification and photo-toxic reactions with drugs and cosmetics [74].

UPF value measured by calculating mean of percentage transmission in UVA and UVB region using the following equation [75].

$$UPF = \frac{\sum_{\lambda=280}^{400} E\lambda S\lambda \Delta\lambda}{\sum_{\lambda=280}^{400} E\lambda\, S\lambda\, T\lambda \Delta\lambda}$$

Where,
Eλ = relative erythemal spectral effectiveness
Sλ = solar spectral irradiance
Tλ = average spectral transmission of the specimen
$\Delta\lambda$ = measured wavelength interval (nm)

Table 7 shows UPF ratings and UVA and UVB blocking values of dyed substrate. A molecules contains benzophenone as core moiety and it known for its photo stabilizer property.

3.6 DFT study

In order to evaluate and correlated experimental observations with theoretical calculations DFT computations were performed. We have evaluated azo-hydrazone tautomerization [76], stable tautomeric forms and correlated photophysical interpretations with the DFT calculations.

3.6.1 Geometry optimization

To know the insight details of the azo and hydrazone forms geometries, computational calculations were performed by using DFT (B3LYP /6-31G(d)). Azo and

Table 7 UPF rating and UVA/UVB blocking in comparison with blank dyed fabric

Dye	PET			Nylon			Acrylic		
	UPF rating	UVA Blocking (%)	UVB Blocking (%)	UPF rating	UVA Blocking (%)	UVB Blocking (%)	UPF rating	UVA Blocking (%)	UVB Blocking (%)
Blank	17	95.58	88.01	15	66.87	67.58	20	91.58	95.90
4a	22	95.16	95.38	17	74.81	74.74	50	97.56	97.94
4b	21	94.96	95.08	15	65.87	66.14	37	96.78	97.47
4c	23	94.97	95.33	17	63.10	63.27	33	96.25	97.17
5a	17	92.89	94.33	16	65.07	65.23	37	96.40	97.35
5b	17	93.02	94.07	15	66.60	67.18	25	94.37	96.36
5c	18	93.64	94.44	16	65.68	66.26	30	95.17	96.57

Rating* (15–24 good protection, 25–39 very good protection, 40–50, 50+ excellent protection)
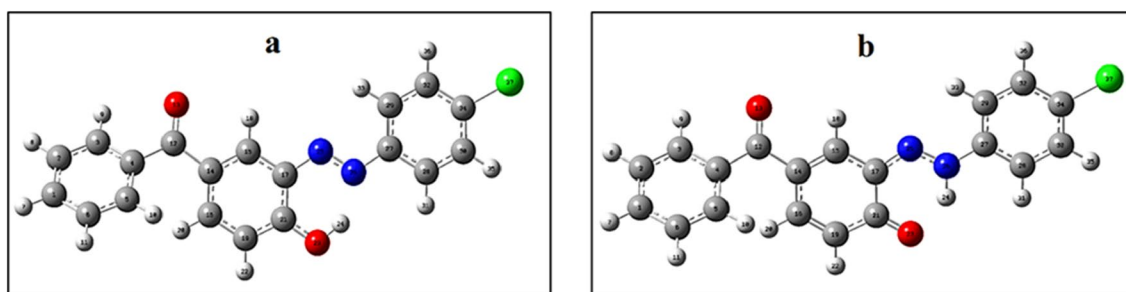
Fig. 12 Optimized geometry of **4b** (**a**) Azo isomer (**b**) Hydrazone isomer using B3LYP/6-31G(d) level

Table 8 Bond lengths of between selected atoms of tautomeric forms (**4aA**–**4cA** and **4aH**–**4cH**)

Compound name	N=N bond length (Å)	O–H bond length (Å)	N–H bond length (Å)	N atom no	H atom no
4aA	1.2695	1.00099	1.71397	26	24
4aH	1.29317	1.70561	1.04186	26	24
4bA	1.27002	0.99981	1.72011	26	24
4bH	1.2952	1.70376	1.04188	26	24
4cA	1.2715	0.99926	1.72326	26	24
4cH	1.30214	1.72029	1.03922	26	24

Table 9 Calculated energies of tautomeric forms at B3LYP/6-31G(d) in $CHCl_3$

Compound name	E/Hartree	$\Delta E/kJ\ mol^{-1}$	ΔG/Hartree
4aA	−992.078	0	−992.144639
4aH	−992.0761	4.776694	−992.14282
4bA	−1451.682	0	−1451.751916
4bH	−1451.6794	7.06394	−1451.749226
4cA	−1196.5751	0	−1196.648555
4cH	−1196.5737	4.603378	−1196.646802

hydrazone forms optimized geometries at Ground state indicated alteration in bond lengths. Optimized geometries of dye **4b** azo-hydrazone forms at ground state in chloroform confirms tautomerization in the dye (Fig. 12).

Further evaluation of aza-hydrazone tautomerism based on bond distances between the selected atoms of the dyes were done (Table 8). **–N=N–** bond distances

have been increased from **1.2695–1.2715 Å** in azo form to **1.29317–1.30214 Å** in hydrazone form. **–OH** bond lengths also increased from **0.99926–1.00099 Å** in azo forms to **1.70376–1.72029 Å** in hydrazone form. Similarly, **–NH** bond length get reduced from **1.71397–1.72326 Å** of azo forms to **1.03922–1.04188 Å** of hydrazone form suggesting clearly the existence of two forms.

3.6.2 Electronic energies of tautomeric forms

Two divergent peaks of absorption spectra for these dyes indicate two tautomeric forms, so one can study comparative stabilities of the tautomer forms. Electronic energies of optimized azo forms and respective hydrazone forms in chloroform have been matched using B3LYP functional 6-31G(d) basis set. It is clearly noticeable that all the azo forms of dyes are comparatively more stable than their respective hydrazone forms by 4.60–7.06 kJ mol^{-1} (Table 9).

3.7 TD-DFT computations

The optimized ground state geometries of the dyes in various polarities solvents were exposed to TD-DFT with B3LYP functional and 6-31G (d) basis set level. As minimum as ten excited states considered for each dye. Absorption maxima, oscillator strengths, vertical excitations, and corresponding orbital contributions in chloroform were recorded (Table 10). DFT and TD-DFT outcomes advise that there is noticeable impact of donating moieties on the absorption of the dyes. Computationally obtained values for the dyes are in decent agreement with experimental interpretations.

Table 10 Observed UV-visible absorption and computed absorption spectral data at B3LYP/6-31G (d) for all dyes in chloroform

Experimental				Theoretical			
Compound	λ_{max} (nm)	Ɛ Molar absorptivity (dm^3 mol^{-1} cm^{-1})	Oscillator strength (f)	Vertical excitation (nm)	Energy (eV)	Oscillator strength (f)	Orbital contribution (%)
4aA	322	33,511	0.3588	326	3.8019	0.3498	H->L (95)
4aH	372	18,619	0.1713	360	3.4447	0.1896	H->L (91)
4bA	332	27,671	0.8302	352	3.5195	0.8267	H->L (98)
4bH	378	17,040	0.1417	399	3.1082	0.1327	H->L (89)
4cA	326	15,296	0.1579	349	3.5522	0.1485	H->L (97)
4cH	378	5079	0.0409	374	3.3183	0.0457	H->L (90)
5aA	351	13,944	0.2563	359	3.4557	0.2398	H->L (96)
5bA	360	8993	0.1564	368	3.3677	0.1731	H->L (95)
5cA	376	3697	0.0633	362	3.4226	0.0313	H->L (99)

λmax = Experimental maximum wavelength, *f* = Oscillator strength
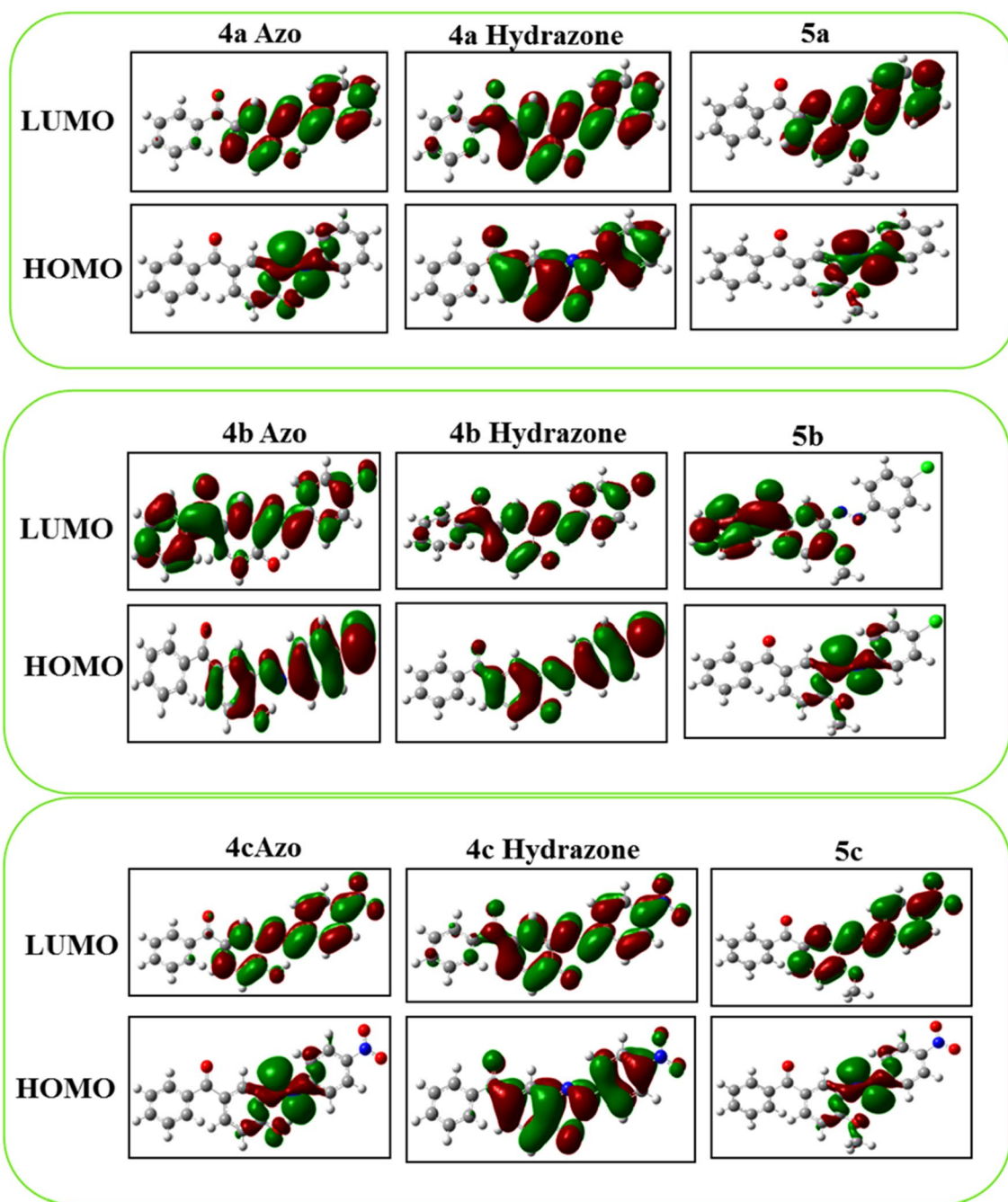
Fig. 13 Frontier molecular orbitals diagrams in CHCl$_3$ optimized at B3LYP/ 6-31G(d) level. Optimized structure of 4b at B3LYP/6-31G(d) level (a) Azo form (b) Hydrazone form

3.7.1 Frontier Molecular orbitals

Electronic density distributions at highest occupied molecular orbital level (HOMO) and at lowest unoccupied molecular orbital level (LUMO) were assessed through Frontier Molecular Orbitals during excitations. Electron density distribution for azo forms **(4aA, 4bA and 4cA)** and corresponding methoxy analogues **(5a,**

5b and 5c) are situated mostly on –N=N– core which is slightly shifted to hydroxyaryl core resulting into less charge transfer and are in good agreement with the spectral data (Fig. 13).

On the other hand, electronic density at HOMO of hydrazone forms **(4aH, 4bH and 4cH)** is situated mostly on–N=N– core and adjacent phenyl moieties which get transferred to the carbonyl of benzophenone

Fig. 14 HOMO–LUMO energy gap in CHCl$_3$ optimized at B3LYP/6-31G(d) level
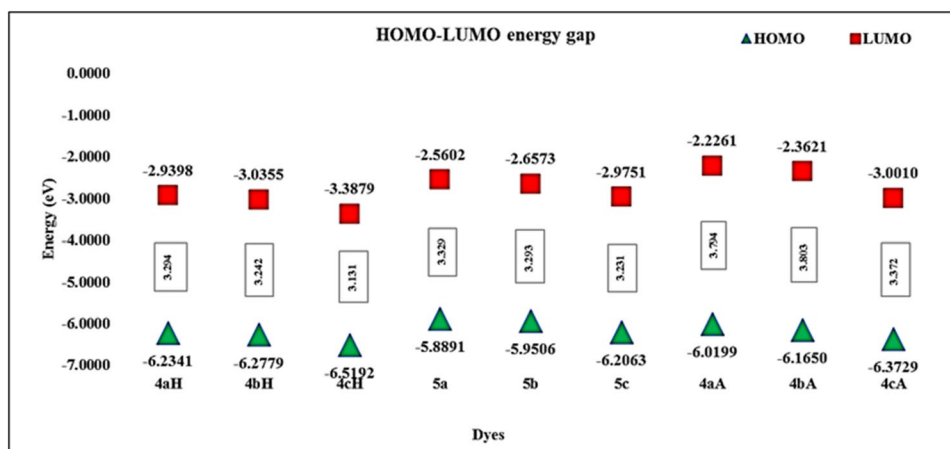
core resulting into more red shift in the photophysical properties.

3.7.2 HOMO–LUMO energy gap

HOMO and LUMO energy band gaps of dyes **4aH, 4bH and 4cH** hydrazone are lowered than the corresponding optimized azo forms **(4aA, 4bA and 4cA)** and methoxy forms **(5a, 5b and 5c)** supported red shifted absorption maxima. Moreover, energy separation between HOMO and LUMO levels follow the same trends suggested large Stokes shift in the hydrazone-form of dyes in comparison to their corresponding azo analogues.–NO$_2$ substituted dyes **(4cA, 4cH and 5c)** are having more red shift than –Cl substituted **(4bA, 4bH and 5b)** dyes than unsubstitued **(4aA, 4aH and 5a)** dyes (Fig. 14).

3.8 Electrophilicity index

Stability of dyes were estimated mathematically by means of computationally gathered electronic energies at B3LYP/6-31G (d) level. So, ω (electrophilicity index) was utilized. Parr et al. defined the electrophilicity-index as the measurement of tendency of the group to absorb electrons and is mathematically expressed as [77, 78]:

$$\omega = \frac{\mu^2}{2\eta} \tag{4}$$

Where,
ω = electrophilicity-index
μ = chemical-potential
η = chemical-hardness
Chemical-hardness and chemical-potential determined by using the following equations:

$$\mu = -\frac{(IP + EA)}{2}$$

$$\eta = \frac{(IP - EA)}{2}$$

Where,
IP = ionization potential, (energy change to the system when an electron is get removed)
EA = electron affinity, (energy change to the system when an electron get added)
But then for finding EA and IP, one can determine three energy values (E_N, E_{N-1} and E_{N+1})
Where,
E symbolises for total energy of a system and N symbolises total electron counts.
Above said methods make the whole system time consuming and monotonous. So alternatively values of chemical hardness and chemical potential can be determined by using Koopmans theorem:

$$\mu = \frac{(E_{LUMO} + E_{HOMO})}{2}$$

$$\eta = \frac{(E_{LUMO} - E_{HOMO})}{2}$$

Where,
E_{LUMO} = energy associated with LUMO
E_{HOMO} = energy associated with HOMO
Also, the Net electrophilicity is expressed as,

$$\omega^{\pm} = \omega^+ + \omega^-$$

Where,

Table 11 Eletrophilicity index of azo and hydrazone forms in chloroform

Dyes	E (kJ mol⁻1)	HOMO	LUMO	Difference	Sum	μ	η	ω	ω⁻	ω⁺	ω±
4aA	−3,263,355.123	−0.22911	−0.09509	0.13402	−0.3242	−0.1621	0.06701	0.19606335	0.0035174	0.0006059	0.0041234
4aH	−3,263,357.122	−0.21643	−0.10804	0.10839	−0.32447	−0.162235	0.054195	0.24282863	0.0025386	0.0006326	0.0031712
4bA	−2,705,423.157	−0.23072	−0.09966	0.13106	−0.33038	−0.16519	0.06553	0.20820797	0.0034883	0.0006509	0.0041391
4bH	−2,705,424.365	−0.21869	−0.11156	0.10713	−0.33025	−0.165125	0.053565	0.25451569	0.0025618	0.0006667	0.0032284
4cA	−2,902,939.964	−0.23959	−0.11934	0.12025	−0.35893	−0.179465	0.060125	0.26783939	0.0034514	0.0008563	0.0043077
4cH	−2,902,941.369	−0.22809	−0.12451	0.10358	−0.3526	−0.1763	0.05179	0.30007424	0.0026944	0.0008029	0.0034973
5a	−3,366,441.826	−0.22124	−0.08181	0.13943	−0.30305	−0.151525	0.069715	0.16466919	0.0034123	0.0004666	0.0038789
5b	−3,366,443.409	−0.22657	−0.08681	0.13976	−0.31338	−0.15669	0.06988	0.17567084	0.0035872	0.0005266	0.0041138

$$\omega^+ = \frac{(E_{LUMO})^2}{2(E_{LUMO} - E_{HOMO})} \tag{5}$$

and

$$\omega^- = \frac{(E_{HOMO})^2}{2(E_{LUMO} - E_{HOMO})} \tag{6}$$

Hence, among possible tautomeric structure's, stable confirmation can be predicted by calculating net elerophilicity index ($\omega^{\pm}$) (Table 11).

4 Conclusion

Dyes **4a**, **4b** and **4c** exhibited dual absorption peaks (azo form and hydrazone forms) and exhibited elivated molar-extinction coefficients as related to corresponding methoxy analogues **5a**–chaving singal absorption. Azo forms (**4aA**, **4bA** and **4cA**) and their methoxy analogues (**5a**–**c**) are less sensitive to the viscosity in varying polarity viscous media (glycerol-dimethylsulfoxide, toluene–polyethylene glycol 400 and toluene-paraffin oil). However, hydrazone forms (**4aH**, **4bH** and **4cH**) exhibited highly viscosity sensitive emission enhancement of (47–96 fold) in varying polarities viscous mixtures as a combined effect of viscosity and H-bonding. Systematic substitutional variations along with comprehensive photophysical characterization of 4-hydroxy benzophenone and corresponding parallel methoxy analogues (4-methoxy benzophenone) dyes allowed to evaluate the role of H-bonding in the emission enhancement. Forster-Hoffman plots showed viscosity sensitivity (x = 0.448–0.697) for hydrazone forms of the dyes (**4aH**, **4bH** and **4cH**). Solvent polarity graphs showed positive solvatochromism for all the dyes. Theoretical calculations by DFT revealed azo-hydrazone tautomerization in 4-hydroxy benzophenone series of dyes. Electrophilicity index calculations and HOMO–LUMO energy levels suggested that hydrazone forms are most stable. TD-DFT, Frontier molecular orbitals and HOMO–LUMO energy gap calculations are in good agreement with the experimentally noticed data.

Compliance with ethical standards

Conflict of Interest The author(s) declare that they have no competing interests.

References

1. Hunger K (2003. ISBN 3-527-30426-6; Journal of the American Chemical Society 2003;125:10144–10144) Industrial dyes: chemistry, properties, applications Edited by Klaus Hunger (Kelkheim, Germany). Wiley-VCH, Weinheim. https://doi.org/10.1021/ja0335418

2. Sancho MI, Jubert AH, Blanco SE, Ferretti FH, Castro EA (2008) Determination of dissociation constants of p-hydroxybenzophenone in aqueous organic mixtures—solvent effects. Can J Chem 86:462–469. https://doi.org/10.1139/v08-040

3. Patel HM (2014) Synthesis, structure investigation and dyeing assessment of novel bisazo disperse dyes derived from UV absorbing material. IOSR J Appl Chem 6:51–55

4. Jiang X, Rui Y, Chen G (2009) Improved properties of cotton by atmospheric pressure plasma polymerization deposition of sericin. J Vinyl Addit Technol 21:129–133. https://doi.org/10.1002/vnl

5. Patel HM, Dixit BC (2014) Synthesis, characterization and dyeing assessment of novel acid azo dyes and mordent acid azo dyes based on 2-hydroxy-4-methoxybenzophenone-5-sulfonic acid on wool and silk fabrics. J Saudi Chem Soc 18:507–512. https://doi.org/10.1016/j.jscs.2011.10.015

6. Dixit B, Patel H, Desai D (2007) Synthesis and application of new mordent and disperse azo dyes based on 2,4-dihydroxybenzophenone. J Serb Chem Soc 72:119–127. https://doi.org/10.2298/JSC0702119D

7. Youssef BM, Ahmed MHM, Arief MMH, Mashaly HM, Abdelghaffar RA, Mahmoud SA (2014) Synthesis and application of functional (Anti-UV) azo-dyes based on γ-acid on wool fabrics. Indian J Sci Technol 7:1005–1013

8. Kiguchi M, Evans P, Ekstedt J, Williams R, Kataoka Y (2001) Improvement of the durability of clear coatings by grafting of UV-absorbers on to wood. Surface Coat Int Part B: Coat Trans 84:263–270. https://doi.org/10.1007/BF02700407

9. Allen NS (2008) Photofading mechanisms of dyes in solution and polymer media. Rev Progr Color Re Top 17:61–71. https://doi.org/10.1111/j.1478-4408.1987.tb03752.x

10. Kehayoglou AH, Tsatsaroni EG, Kehayoglou AH, Eleftheriadis IC, Kyriazis LE (1998) Effectiveness of various UV-absorbers on the dyeing of polyester with disperse dyes. Part IV. Dyes Pigments 38:65–75. https://doi.org/10.1016/S0143-7208(97)00085-5

11. Kehayoglou AH, Tsatsaroni EG, Eleftheriadis IC, Loufakis KC, Kyriazis LE (1997) Effectiveness of various UV-absorbers in dyeing of polyester with disperse dyes. Part III. Dyes Pigments 34:207–218

12. Tsatsaroni EG, Kehayoglou AH (1995) Dyeing of polyester with CI disperse yellow 42 in the presence of various UV-absorbers. Part II. Dyes Pigments 28:123–130. https://doi.org/10.1016/0143-7208(95)00007-3

13. Tsatsaroni EG, Eleftheriadis IC (2004) UV-absorbers in the dyeing of polyester with disperse dyes. Dyes Pigments 61:141–147. https://doi.org/10.1016/j.dyepig.2003.10.002

14. Freeman HS, Posey JC (1992) An approach to the design of lightfast disperse dyes—analogs of disperse yellow 42. Dyes Pigments 20:171–195

15. Bhide R, Jadhav AG, Sekar N (2016) Light fast monoazo dyes with an inbuilt photostabilizing unit: synthesis and computational studies. Fibers Polym 17:349–357. https://doi.org/10.1007/s12221-016-5717-3

16. Dixit BC, Patel HM, Desai DJ, Dixit RB (2009) Studies on dyeing performance of novel acid azo dyes and mordent acid azo dyes based on 2,4-dihydroxybenzophenone. E-J Chem 6:315–322

17. Athalye A (2015) Automotive textiles. Int J Textile Eng Processes 1:42–52

18. Zimniewska M. Innovations in UV protection by textiles 2015:35.

19. Farzana N (2015) Fluorescent disperse dyes reflectance spectra, relative strength and performance evaluation of coumarin class on polyester/cotton blended fabric. Int J Res Eng Technol 4:488–494

20. Maqbool H, Ganesh SD, Pai VK (2013) Studies on physicochemical properties of azo cardanol sulfonates and their salts. Der Pharma Chem 5:154–159

21. Szuster L, Kaźmierska M, Król I (2004) Fluorescent dyes destined for dyeing high-visibility polyester textile products. Fibres Textiles Eastern Europe 12:70–75

22. Yang P, Kokot S (1996) Thermal analysis of different cellulosic fabrics. J Appl Polym Sci 60:1137–1146. https://doi.org/10.1002/(SICI)1097-4628(19960523)60:8<1137::AID-APP6>3.0.CO;2-M

23. Barsotti F, Brigante M, Sarakha M, Maurino V, Minero C, Vione D (2015) Photochemical processes induced by the irradiation of 4-hydroxybenzophenone in different solvents. Photochem Photobiol Sci 14:2087–2096. https://doi.org/10.1039/c5pp00214a

24. Bhasikuttan C, Singh K, Palit DK, Sapre V, Mittal JP (1998) Laser flash photolysis studies on the monohydroxy derivatives of benzophenone. J Phys Chem A 5639:3470–3480 doi: S1089-5639(97)02375-X CCC

25. Das PK, Encinas MV, Scaiano JC (1981) Laser flash photolysis study of the reactions of carbonyl triplets with phenols and photochemistry of p-hydroxypropiophenone. J Am Chem Soc 103:4154–4162. https://doi.org/10.1021/ja00404a029

26. Palit DK (2005) Photophysics and excited state relaxation dynamics of p-hydroxy and p-amino-substituted benzophenones: a review. Res Chem Intermediates 31:205–225. https://doi.org/10.1163/1568567053147020

27. Barsotti F, Ghigo G, Berto S, Vione D (2017) The nature of the light absorption and emission transitions of 4-hydroxybenzophenone in different solvents. A combined computational and experimental study. Photochem Photobiol Sci. https://doi.org/10.1039/C6PP00272B

28. Yoshino J, Kano N, Kawashima T (2013) Fluorescent azobenzenes and aromatic aldimines featuring an N–B interaction. Dalton Trans:15826–15834. https://doi.org/10.1039/c3dt51689j

29. Saylam A, Seferoğlu Z, Ertan N (2014) Azo-8-hydroxyquinoline dyes: the synthesis, characterizations and determination of tautomeric properties of some new phenyl- and heteroarylazo-8-hydroxyquinolines. J Mol Liq 195:267–276. https://doi.org/10.1016/j.molliq.2014.02.027

30. Satam MA, Raut RK, Sekar N (2013) Fluorescent azo disperse dyes from 3-(1,3-benzothiazol-2-yl)naphthalen-2-ol and comparison with 2-naphthol analogs. Dyes Pigments 96:92–103. https://doi.org/10.1016/j.dyepig.2012.07.019

31. Puchtler H, Sweat F, Gropp S (1967) An investigation into the relation between structure and fluorescence of azo dyes. J Royal Microsc Soc 87:309–328. https://doi.org/10.1111/j.1365-2818.1967.tb04513.x

32. Wakatsuki Y, Yamazaki H, Grutsch PA, Santhanam M, Kutal C (1985) Study of intramolecular sensitization and other excited-state pathways in orthometallated azobenzene complexes of Palladium (II). J Am Chem Soc 4:8153–8159. https://doi.org/10.1021/ja00312a057

33. Shimomura M, Kunitake T (1987) Fluorescence and photoisomerization of azobenzene-containing bilayer membranes. J Am Chem Soc 33:5175–5183. https://doi.org/10.1021/ja00251a022

34. Ghedini M, Pucci D, Crispini A, Aiello I, Barigelletti F, Gessi A (1999) Dinuclear cyclopalladated azobenzene complexes: a comparative study on model compounds for organometallic liquid-crystalline materials. Appl Organomet Chem 13:565–581. https://doi.org/10.1002/(SICI)1099-0739(199908)13:8<565::AID-AOC891>3.0.CO;2-C

35. Han M, Hara M (2005) Intense Fluorescence from light-driven self-assembled aggregates of nonionic azobenzene derivative. J Am Chem Soc 127:10951–10955. https://doi.org/10.1021/ja0509275

36. Aiello I, Ghedini M, La Deda M (2002) Synthesis and spectroscopic characterization of organometallic chromophores for photoluminescent materials: cyclopalladated complexes. JOL 96:249–259. https://doi.org/10.1016/S0022-2313(01)00229-0

37. Han MR, Hara M (2006) Chain length-dependent photoinduced formation of azobenzene aggregates. N J Chem:1–5. https://doi.org/10.1039/b511462d

38. Kano N, Yamamura M, Kawashima T (2015) 2,2'-Disilylazobenzenes featuring double intramolecular nitrogensilicon coordination: a photoisomerizable fluorophore. Dalton Trans 44:16256–16265. https://doi.org/10.1039/C5DT02038G

39. Warde U, Sekar N (2017) NLOphoric mono-azo dyes with negative solvatochromism and in-built ESIPT unit from ethyl 1,3-dihydroxy-2-naphthoate: estimation of excited state dipole moment and pH study. Dyes Pigments 137:384–394. https://doi.org/10.1016/j.dyepig.2016.10.032

40. Jadhav AG, Kothavale S, Sekar N (2017) Red emitting triphenylamine based rhodamine analogous with enhanced Stokes shift and viscosity sensitive emission. Dyes Pigments 138:56–67. https://doi.org/10.1016/j.dyepig.2016.11.021

41. Mallion KB, Turner RW, Todd AH. United States Patent 0 "ice 3,714,16, 1967.

42. Du H, Kim C, Corradini MG, Ludescher RD, Rogers MA (2014) Micro-viscosity of fluid oil confined in colloidal fat crystal networks. Soft Matter 10:8652–8658. https://doi.org/10.1039/C4SM01632G

43. Hazen T, Wuertz S (2004) Environmental biotechnology. Curr Opin Biotechnol 23:414

44. Malomo D, Abimbade SA, Oluwaseun AK (2017) Likely mechanism of dye adhesion on fabrics 1. Likely Mech Dye Adhes Fabrics:9–15

45. Ludescher RD, Jennifer S, Komaiko MGC (2012) Monoazo dyes as probes for bulk and local viscosity. Agro Food Ind Hi Tech 23:12–14

46. Cembran A, Bernardi F, Garavelli M, Gagliardi L, Orlandi G (2004) On the Mechanism of the cis–trans isomerization in the lowest electronic states of azobenzene: S0, S1, and T1. J Am Chem Soc 126:3234–3243. https://doi.org/10.1021/ja038327y

47. Rau H (1973) Spectroscopic properties of organic azo compounds. AngewChemInternatEdit 12:224–235

48. Laikhter A, City I, Behlke MA, Roberts W, City I. (19) United States (12) 2009;1.

49. Bloomfield A, Dewan RK (1971) Viscosity of liquid mixtures. J Phys Chem 75:3113–3119

50. Frisch MJ, Trucks GW, Schlegel HB, Scuseria GE, Robb MA, Cheeseman JR et al (2009) Gaussian 09, Revision C.01. Gaussian 09, Revision B01. Gaussian, Inc., Wallingford, CT

51. Becke AD (1993) Density-functional thermochemistry. III. The role of exact exchange. J Chem Phys 98:5648. https://doi.org/10.1063/1.464913

52. Becke AD (1988) Density-functional exchange-energy approximation with correct asymptotic behavior. Phys Rev A 38:3098–3100. https://doi.org/10.1103/PhysRevA.38.3098

53. Zhao Y, Truhlar DG (2008) The M06 suite of density functionals for main group thermochemistry, thermochemical kinetics, noncovalent interactions, excited states, and transition elements: two new functionals and systematic testing of four M06-class functionals and 12 other function. Theor Chem Accounts 120:215–241. https://doi.org/10.1007/s00214-007-0310-x.

54. Otutu JO, Efurhievwe EM (2013) Synthesis of heterocyclic monoazo disperse dyes derived from 4-Amino-2-chloro-6, 7-dimethoxyquinazoline. J Appl Sci 13:924–928. https://doi.org/10.3923/jas.2013.924.928

55. Ezeribe AI, Bello KA, Adamu HM, Chindo I, Boryo YD (2013) Synthesis and dyeing properties of novel bifunctional reactive bromophenyl-1,3-thiazol-2-amine on nylon fabric. Am J Eng Res 3:52–61. https://doi.org/10.5901/ajis.2014.v3n5p125

56. Ziegler E, Zigeuner G (1949) Spaltungen mittels diazoniumverbindungen. Sci Pharm 17:113–117

57. Patil SR, Choudhary AS, Sekar N (2015) Disperse styryl and azo dyes for polyester and nylon fibre: synthesis, optical properties having the 1,2,4-triketo naphthoquinone skeleton. Fibers Polym 16:1068–1074. https://doi.org/10.1007/s12221-015-1068-8

58. MacNeil JD, Safe S, Hutzinger O (1976) The ultraviolet absorption spectra of some chlorinated biphenyls. Bull Environ Contam Toxicol 15:66–77. https://doi.org/10.1007/BF01686197

59. Brown WG, Reagan H (1947) Steric effects in the ultraviolet absorption spectra of aromatic nitro compounds. J Am Chem Soc 69:1032–1033. https://doi.org/10.1021/ja01197a016

60. Anpo M, Kamat PV (2010) Nanostructure science and technology. In: Masakazu Anpo PVK (ed) Enviromentally benign photocatalysts: applications of titanium oxide-baseed materials. Springer Science & Business Media, p 382

61. Johnston LJ, Hugnot DJ, Wintgen VG (1988) Diphenylketyl radicals: spectroscopy, kinetics, and mechanisms. J Am Chem Soc 110:518–524

62. Tredwell CJ (1980) Viscosity dependent internal conversion in the rhodamine dye, fast acid violet 2R. J Chem Soc Faraday Trans II 76:1627–1637. https://doi.org/10.1039/f29807601638

63. Das K, Sarkar N, Ghosh AK, Majumdar D, Nath DN (1994) Excited-state intramolecular proton transfer in 2-(2'-Hydroxyphenyl) benzimidazole and—benzoxazole: effect of rotamerism and hydrogen bonding. J Phys Chem 1:9126–9132. https://doi.org/10.1021/j100088a006

64. Biczok L, Berces T, Inoue H (1999) Effects of molecular structure and hydrogen bonding on the radiationless deactivation of singlet excited fluorenone derivatives. Chem Eur J 103:3837–3842. https://doi.org/10.1021/jp990208a

65. Martin MM (1975) Hydrogen bond effects on radiationless electronic transitions in xanthene dyes. Chem Phys Lett 35:105–111. https://doi.org/10.1016/0009-2614(75)85598-9

66. Mashaly HM, Abdelghaffar RA, Kamel MM, Youssef BM (2014) Dyeing of polyester fabric using nano disperse dyes and improving their light fastness using ZnO nano powder. Indian J Sci Technol 7:960–967

67. Lee M, Lee MS, Wakida T, Tokuyama T, Inoue G, Ishida S (2005) Chemical modification of nylon 6 and polyester fabrics by ozone-gas treatment. J Appl Polym Sci 100:1344–1348. https://doi.org/10.1002/app.23382

68. Merian E, Carbonell J (1963) UL and VS. The saturation values, rates of dyeing, rates of diffusion, and migration of disperse dyes on heat-set polyester fibers. J Soc Dye Colour 79:505–514

69. Otutu JO (2013) Synthesis and properties of some hetaryl disazo and trisazo disperse dye derivatives of 2-Amino-5-nitrothiazole and 1-naphthylamine. Int J Recent Res Appl Studies 15:197–202

70. Sartori MF (2008) Spectral and fastness properties of benzothiazolylazo dyes. J Soc Dye Colour 83:144–146. https://doi.org/10.1111/j.1478-4408.1967.tb02756.x

71. Deshmukh MS, Sekar N (2014) A combined experimental and TD-DFT investigation of three disperse azo dyes having the nitroterephthalate skeleton. Dyes Pigments 103:25–33. https://doi.org/10.1016/j.dyepig.2013.10.035

72. Ezeribe AI, Bello KA, Adamu HM, Chindo I, Boryo YD (2013) Synthesis and dyeing properties of novel bifunctional reactive bromophenyl-1,3-thiazol-2-amine on nylon fabric. Am J Eng Res 02:52–61

73. Becerir B, Alpay HR. Ultraviolet (UV) protection of textiles: a review. International Scientific Conference 19–20 November 2010, Gabrovo, 2010, p. 301–11

74. Krzysztof K, Barbara LS (2014) Effect of selected metrological parameters of dyed polyester textiles on their UV-barrier properties. Fibers Polym 15:2077–2085. https://doi.org/10.1007/s12221-014-2077-8

75. Hustvedt G, Crews P (2005) The ultraviolet protection factor of naturally-pigmented cotton. J Cotton Sci 9:47–55

76. Saylam A, Seferoglu Z, Ertan N (2008) Synthesis and spectroscopic properties of new hetarylazo 8-hydroxyquinolines from some heterocyclic amines. Dyes Pigments 76:470–476. https://doi.org/10.1016/j.dyepig.2006.10.005

77. Shinde S, Sekar N (2019) Synthesis, spectroscopic characteristics, dyeing performance and TD-DFT study of quinolone based red emitting acid azo dyes. Dyes Pigments 168:12–27. https://doi.org/10.1016/j.dyepig.2019.04.028

78. Parr RG, Szentpaly LV, Liu S (1999) Electrophilicity index. J Am Chem Soc 121:1922–1924. https://doi.org/10.1021/ja983494x

Publisher's Note Springer Nature remains neutral with regard to jurisdictional claims in published maps and institutional affiliations.